Testing Effective Kidney Stone Fragmentation

Johan Markus Steinholt

Norwegian University of Science and Technology
Department of Engineering Cybernetics

Testing effective kidney stone fragmentation

Johan Markus Steinholt
johan.m.steinholt@gmail.com

Counselor:
Adjunct Associate Professor Geir Mathisen, NTNU

Trondheim, June 2013

DEPARTMENT OF ENGINEERING CYBERNETICS
FACULTY OF INFORMATION TECHNOLOGY, MATHEMATICS AND
ELECTRICAL ENGINEERING

NTNU
Norges teknisk-naturvitenskapelige
universitet

Fakultet for informasjonsteknologi,
matematikk og elektroteknikk
Institutt for teknisk kybernetikk

HOVEDOPPGAVE/MASTER THESIS

Kandidatens navn: **Johan Markus Steinholt**

Fag: **Teknisk kybernetikk/Engineering Cybernetics**

Oppgavens tittel (norsk): **Uttesting av effektiv knusing av nyrestein**

Oppgavens tittel (engelsk): **Testing effective kidney stone fragmentation**

Oppgavens tekst:

Through several project- and master theses, NTNU has, in cooperation with St. Olavs Hospital has examined how kidney stone fragmentation with ESWL can be improved. The goal of this work is that an effective fragmenting is to be accomplished, such that the sizes of the fragments are small enough to be passed naturally.

In this context, we wish to study parameters affecting effective fragmentation and to verify the effectiveness of the fragmentation in a controlled environment

Oppgaven består av følgende 3 punkter:

1. Perform a literature study to see which parameters affect kidney stone fragmentation with ESWL.

2. Propose a test setup to verify the effectiveness of kidney stone fragmentation.

3. If time is sufficient, realize the test setup and perform measurements which underpin / demonstrate the methods of kidney stone fragmentation.

Oppgaven gitt: 15. January, 2013
Besvarelsen leveres: 10. June, 2013

Utført ved Institutt for Teknisk kybernetikk

Trondheim, den 15.01.2013

Geir Mathisen
Faglærer

Abstract

During extracorporeal shock wave lithotripsy, kidney stone move-
ment causes a significant amount (more than 50%) of treatment energy
to miss the stone. It is desirable to deveop a system that is able to track
the stone and control the lithotriptor to ensure that all shock waves hit
their target. The goals of this thesis were to examine what parameters
affect kidney stone fragmentation during ESWL and to develop a test
setup for evaluating methods of ESWL treatment. Building on exixting
tracking software and test components developed in past project and
master theses, the test setup was completed. An ESWL control unit
was developed, utilizing an ECG interface to the lithotriptor. A kidney
simulator tank previously developed was augmented and model stones
were produced. The tracking system requires prediction to accurately
estimate the stones position because of delays in the modules of the
test setup, so these delays were identified experimentally. The impact
of movement on fragmentation efficiency were examined through frag-
mentation tests on model stones in the test system. The functionality
of the new modules in the test system were verified on a lithotriptor
at St. Olavs Hospital. Results show that the delay of the total sys-
tem is approx 300 ms with some jitter. Results from the fragmentation
tests suggest that stone movement sigificantly affects fragmentation effi-
ciency. A moving stone receives less shock wave energy, and is therefore
less fragmented. A system which can ensure a high hit percentage will
therefore make treatment more efficient than during normal practice.

Sammendrag

Ved ESWL-behandling forårsaker steinbevegelser at en signifikant mengde (mer enn 50%) av energien i sjokkbølgene ikke treffer steinen. Det er ønskelig å utvikle et system som er i stand til å spore steinen og styre ESWL-apparatet, for å sikre at alle sjokkbølgene treffer målet. Målene med denne oppgaven var å undersøke hvilke parametere som påvirker nyresteinknusing under ESWL, og å utvikle et testoppsett for å kunne evaluere knusemetoder i ESWL. Tracking-software og testutstyr utviklet i tidligere master- og prosjektoppgaver ble inkorporert i et komplett testoppsett. En ESWL-styreenhet som baserer seg på apparatets EKG-interface, ble utviklet. En nyresimulator-tank som ble utviklet i en tidligere prosjektoppgave ble forbedret, og nyresteinmodeller ble produsert. Tracking-systemet er avhengig av prediksjon for å kunne estimere nyresteinens posisjon på grunn av forsinkelser gjennom testoppsettets moduler. Derfor ble forsinkelsen i modulene funnet eksperimentelt. Steinbevegelsens innvirkning på effektiviteten av knusing ble undersøkt gjenom tester på modellsteiner i testoppsettet. Funksjonaliteten til de nye modulene som ble utviklet til testoppsettet ble verifisert på ESWL-utstyr ved St. Olavs Hospital. Resultater viser at forsinkelsen gjennom hele testsystemet er ca 300 ms med noe "jitter". Resultater fra testene av knusing indikerer at steinbevegelse har en signifikant innvirkning på knusingens effektivitet, en stein i bevegelse blir truffet av færre sjokkbølger og blir derfor mindre knust. Et system som kan sikre at en høy prosentandel av sjokkbølger treffer steinen, vil derfor gjøre behandlingen mer effektiv enn den er i dag.

Preface

This master thesis is the last piece of work for the Engineering Cybernetics Master program at NTNU. Working with this topic has been interesting and challenging. It has been a combination of several, very different topics such as medicine, programming, electronics and practical work. This combination has made working on this thesis fun, and I have been able to aquire a lot knowledge in new fields of science and technology.

Many people have helped and guided me through this process and I would like to give some of them a special thanks; Dr. Ingrid Høye, Dr. Carl-Jørgen Arum and Bjørn Lindvåg at St. Olavs Hospital for participating in this project, assisting me in tests on their equipment (even outside of regular working hours), and providing valuable feedback. Ole-Vegard Solberg, Tormod Selbakk and Christian Askeland at SINTEF lending of equipment. Geir Mathisen, my guidance counselor for good feedback, suggestions and motivation for this project. I would also like to thank my fellow students at office D252 for making this semester very enjoyable.

Contents

Nomenclature

ESWL	Extracorporeal Shock Wave Lithotripsy
In Vitro	Outside of the body (in a test setup)
In Vivo	Inside the body (may be test setup with, for instance, animal organs)
Lithotripsy	Medical procedure involving the physical destruction of hardened masses like kidney stones (Wikipedia)
Lithotriptor	The equipment used for lithotripsy

1 Introduction

This master thesis presents work done on a system designed to improve kidney stone treatment by ESWL (Extra-corporeal Shock Wave Lithotripsy). In 2010, Jens Kristian Tøraasen[44] developed tracking software using image analysis done on ultrasound images. This work was continued by Jens Runnestø in 2011[36][35]. The author continued the work in 2012[40] and integrated a real-time ultrasound interface into the tracking program.

The aim of this thesis is examine what parameters affect the fragmentation process and to complete the test setup for evaluating the performance of the tracking system. This section presents the motivation behind these tasks, details about the previous work done on this system, limitations in this project and an outline of the report.

1.1 Motivation

ESWL aims to fracture kidney stones using ultrasonic sound waves. The generator emitting these waves are usually aimed manually using x-ray or ultrasound imaging. The ESWL shock waves are usually released with a frequency of around 90 shots per minute, and several thousand shock waves may be required to break the stone. The kidney and the contained stone are unfortunately not stationary during the treatment. Respiration, patient movement from pain, and stone movement when it fractures causes the shock waves to miss on as many as 50% or more of the shots[33]. This causes damage to surrounding tissue and prolonged treatment time.

In 2010 Tøraasen[44] developed tracking software to be able to eliminate missed shots, using image analysis in ultrasound images. The purpose was to ensure shock waves were only released when the stone was in the focus of the lithotriptor. This work was continued by Runnestø in 2011[35][36]. The two previous master thesis only ran image analysis on pre-recorded videos, so in 2012, the author, Steinholt [40] extended the system to be able to receive ultrasound images in real-time from an interface called Ulterius.

The next step in this process is to examine which parameters affect stone fragmentation in ESWL. To test the effectiveness of fragmentation, a complete test setup is needed. The previous theses have all described the complete system, with varying detail, but all the system components have not yet been developed. The system needs a way of controlling the lithotriptor(treatment device) and model stones to test on. Other components such as the kidney simulator tank, need alterations to be compatible with the treatment equipment. It was determined by Runnestø[35] that some form of prediction is needed to enable

the tracking system to function, so a big part of creating a test setup is to measure or verify the delays of each system module.

The ultimate goal of this topic is to maximize treatment efficiency and minimize tissue damage to the patient.

1.2 Earlier Work

Earlier, two project and two master-theses about real-time tracking of kidney stones have been written. In the spring of 2010, Jens Kristian Tøraasen wrote a master thesis[44] that resulted in software with the ability to track a kidney stone on a video of ultrasound images taken from a real patient, but not in real-time. This program used pre-processing of the image by mean-filtering, thresholding and a tracking algorithm called Mean-Shift. The program was tested on 7 recorded videos from patients at St. Olavs Hospital, and it showed that tracking was possible even when the stone, under certain conditions, moved out of the imaging plane.

After Tøraasens thesis, a project by Jostein Låg Runnestø[35] followed in the fall of 2010. The aim of the project was to develop a movable rig and phantom kidney with a simulated stone to be able to produce realistic ultrasound images under controlled conditions. A box was constructed featuring two servos that could move a model kidney in three dimensions using bendable sticks. The box was also fitted with a membrane designed to mimic the ultrasonic properties of the human abdominal wall. A phantom kidney was developed, using household jelly with a piece of chalk as the kidney stone. Ultrasound images were captured to compare the rig with real images. The box in which the kidney was suspended was filled with water, which causes minimal disturbance in the ultrasound images. The same goes for jelly, so this test rig was made primarily for concept testing. Cornflour was proposed as a possible additive in the water for more realistic scattering in the ultrasound image.

Runnestø continued with a master thesis[36] on this subject in the spring of 2011, where he proposed a setup for the whole system. The goal here, was to connect the ultrasound imaging equipment to a computer running tracking software that simultaneously controls the apparatus for treatment, the ESWL-machine so that it can fire when the stone is confirmed to be in focus. The main purpose of the thesis was to measure the real-time properties of the system, and to develop an estimator to overcome the inevitable delay. Runnestø used a frame grabber to transfer images between the imaging device and the computer, and an Arduino (a simple, microcontroller-based IO-unit) to simulate the ESWL control. He identified a delay and designed predictors to compensate. One based on low pass-filtered extrapolation and another

based on a Kalman-filter. They were tested on the same videos as Tøraasen used for testing and the estimators gave good results on continuous, periodic movements, but gave poor results with uneven movements and when the stone changed direction. The software developed also contained a method of calculating optimal placement of the focal-region of the lithotriptor based on stone movements.

The author made an extension to the tracking system in a project thesis in the fall of 2012 [40]. This enabled images to transfered from an ultrasound scanner in real-time using an interface called Ulterius which is available on some Ultrasonix ultrasound scanners. Ulterius uses a TCP-based protocol to transfer images over an ethernet connection from a server application running on the scanner to a receiving PC. The delay of this image transfer was measured and found to be have a mean value of 255 ms. Test of the tracking system in real-time were also conducted, but these proved inconclusive because of limited time available.

1.3 Limitations

The tracking program mentioned as part of the test setup is based on theory in fields of image analysis and computer vision. This theory is not covered here, for details, refer to the respective theses by Runnestø[36] and Tøraasen[44].

The fragmentation tests presented in this thesis were done using model stones in a kidney simulator tank. The tank membranes were made of a flexible plastic and is not guaranteed to fully mimic the acoustic conditions of the abdominal wall.

The conditions in the kidney simulator tank were ideal compared to real stones in a real patient. In a treatment situation, tissue and air may impair the shock waves and cause less energy to hit the stone. Also, visualizing the stone is much easier in the simulator tank since the stone is surrounded by water which does not scatter ultrasound waves.

The movement of stones in the simulator were designed based on ideal descriptions of real stone movement. These sinusoidial movement patterns may not be the same as in a real treatment situation, where the movement of stones vary from patient to patient. Therefore, fragmentation results may differ depending on the patient. The fragmentation of moving stones were only compared to the fragmentation of the stationary stones in the same simulator, and this difference is used to reason about results in real treatment situations.

The full system was not tested as part of this thesis. The reson being that the simulator tank setup and ultrasound equipment were found to be inadequate.

Since the tests were done in operating rooms at St. Olavs Hospital, limited time was available for setting up tests. Combined with the fact that a lot of time was used overcoming the inaccurate ajustments on the kidney simulator when aiming the lithitriptor, the conclusion was made that full system tests were not feasible. Another reason for not doing full system tests were limitations in the ultrasound equipment. The available probe had a scan depth of only 9 cm, making it hard to create an image of the model stone in the simulator tank (which measures 28 cm across).

1.4 Outline

Section 2 presents a literature review of topics concerning kidney stones and treatment, shock wave theory, stone fragmentation, model stones and tissue damage. The next section, section 3, discusses the parameters of fragmentation and how to achieve effective fragmentation in the context of the lithotriptor at St. Olavs Hospital. Section 4 describes the full test setup for evaluating effective fragmentation, followed by section 5 which describes the design of system modules added to the test setup. Section 6 presents the tests performed on the test setup and on model stones, and the results of these tests are presented in section 7. A discussion of the test setup and delays are found in section 8, and propositions for further work are presented in section 9. Section 10 contains conclusions, followed by references and appendix.

2   Literature Review

This section presents theory relevant for understanding the mechanics of lithotripsy and kidney stone fragmentation. The first part briefly summarizes kidney stones, and stone treatment, followed by an introduction to shock wave accoustics. Section 2.3 presents theories and mechanisms of stone fragmentation, followed by a description of different model kidney stone materials. The end of the section discusses which parameters of ESWL affect fragmentation, and what tissue damage may occur. For an introduction to ESWL technology, refer to the authors project thesis[40].

2.1   Kidney Stones

A brief review of kidney stones are given here. This material is adapted from the authors project thesis[40].

Kidney stone, or urinary calculi, is the term for hard structures of crystals, which occur in the kidney or the ureter[45]. The crystals are formed by precipitation of organic or inorganic salts in the urine. Three types of urinary calculi exist based on the chemical composition of the stone itself, calcium stones, infection stones and organic stones.

Calcium stones are the most common and make up approx. 80% of kidney stones. These stones consist of crystals of calcium oxalate or calcium phosphate and occur because of excretion of calcium in the urine. As a result of a high calcium contents in these stones, they are easily seen in x-ray images.

Infection stones consist of a salt normally not found in urine, but that is a result of an infection, magnesium ammonium phosphate. Such stones are not as hard as calcium stones and are not as visible on x-ray images, therefore, they may have to be diagnosed by other means, such as ultrasound or computer tomography (CT-scan).

Organic stones occur as a result of increased precipitation of organic substances in the urine, caused by metabolic disorders. Only 5-10% of urinary calculi are of this type. These stones may not be visible in x-ray either, and may have to be diagnosed with other means, as mentioned above.

The most common symptom of a kidney stone is pain. This is considered to be among the worst pains we can experience. It is commonly caused by a blockage during stone passage from the renal pelvis to the ureter or further passage within the ureter. When blockage occurs, the pressure inside the kidney and ureter rises and as production of urine continues, this can cause a condition known as renal colic. This is an acute pain in the kidney region and

down to the groin. It is often accompanied by nausea and fever. If the stone obstructs further down in the ureter, an increased need to urinate and pain in the bladder often follows. From figure 1 a kidney with calculi in two different locations can be seen.

Figure 1: Cross-section of kidney with stones calyx and in ureter. From Avant-garde Urology[1]

2.1.1   Treatment of Kidney Stones

Modern treatment of urinary calculi is based on minimally invasive proce-dures, as opposed to traditional methods, such as pyelolithotomy (surgical removal)[42][41]. There are mainly three methods used:

- URS - Ureteroscopy

- PCNL - Percutaneous Nephrolithotomy

- ESWL - Extra corporeal Shock Wave Lithotripsy

URS is done by inserting an instrument up the urethra, through the bladder and up into the ureter to remove the stone.

PCNL is mainly used on large calculi, over 20mm. Instruments are inserted percutaneously (through a hole) into the calyx through which the stone is removed..

ESWL is considered the least invasive method. The procedure consists of send-ing ultrasound shock waves into the body, without any surgery or endoscopy, to fragment the stone into pieces small enough to pass naturally. Zhou et al. states that fragments with a diameter of 2 mm or smaller are considered able to be passed naturally[48]. See figure 2 for illustration.
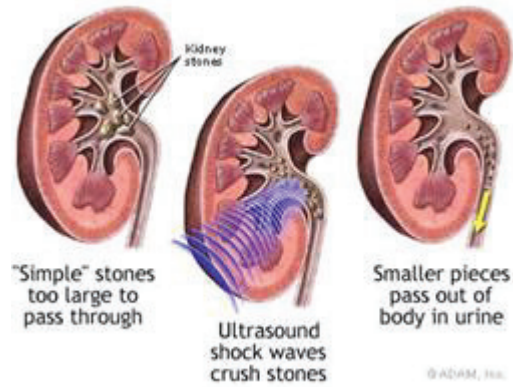
Figure 2: ESWL treatment. Illustration from Avantgarde Urology [1]

For more information about these procedures and their risks, refer to the authors previous thesis[40].

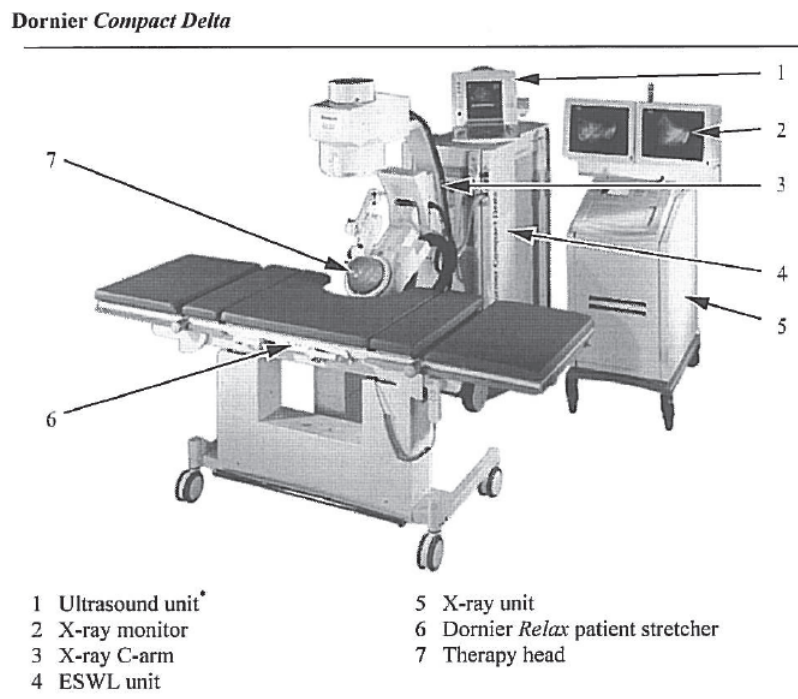An ESWL-treatment system is shown in figure 3.

Figure 3: Dornier Compact Delta ESWL-system. From [2]

2.2 Shock Wave Acoustics of ESWL

To understand how urinary calculi are fragmented by shock waves generated by ESWL-generators, it is important to consider the physics of acoustic waves and shock waves. This will be presented in this section.

2.2.1 Acoustic Waves

When an object moves in a fluid, gas or liquid, acoustic waves are generated [7]. As shown in figure 4, a piston causes compression in a fluid, the compressed region is marked by a darker color. The compressed particles press against ajacent molecules and thus, the wave moves forward as a longitudal wave. An acoustic wave can also be propagation of a low pressure zone, as would be the case if the figure also showed the fluid on the left side of the piston. As the piston moves from left to right, a low pressure is generated at its the previous position, and this propagates to the left as a low pressure wave. A higher pressure wave is called a compressive wave, and a low pressure wave is known as a tensile wave.
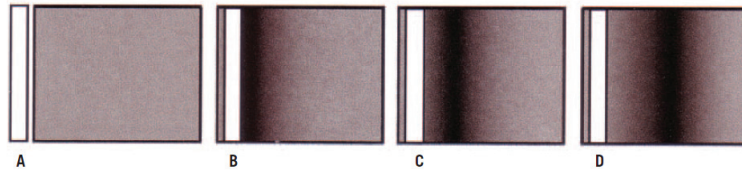

Figure 4: Acoustic wave propagation. [7]

As an acoustic wave propagates, it does not only affect the local fluid pressure, but also the density and particle velocity.

Acoustic impedance is an important characteristic of a material when discussing acoustic waves.

$$Z_0 = \rho_0 c_0 \tag{1}$$

The specific acoustic impedance of a material, Z_0, is defined in equation 1, where ρ_0 is the density of the medium and c_0 is the sound speed in the medium. The units are referred to as Rayls[7]. The impedance is important because it describes the relationship between pressure, density and particle velocity of a wave, and also, affects what happens when an acoustic wave crosses the boundary of two materials with different characteristics. When this happens, part of the wave is reflected back and the rest continues into the new medium. The amount of energy that is reflected and the amount that continues can

8

be described by the energy transmission and reflection coefficients T_I and R_I respectively, described by equation 2.

$$T_I = \frac{4Z_1Z_2}{(Z_2 + Z_1)^2} = 1 - R_I \tag{2}$$

Z_1 and Z_2 are the acoustic impedances of the material the wave transitions *from* and *to*.

In the context of shock wave lithotripsy, these coefficients describes how much energy will reach the calculi after transitioning from the generator to tissue, through the body and finally into the stone itself.
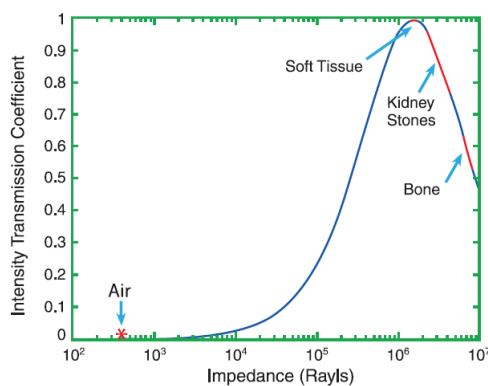

Figure 5: Transmission coefficients for transmission from water into materials with different impedances [7]

Most lithotripters generate the shock waves in a fluid filled ellipsoid structure. The shock waves are transmitted into soft tissue through a ball-shaped treatment head that is in direct contact with the patients body. From figure 5 it can be seen that a transition from water directly into soft tissue implies very little energy loss due to reflection, with a transmission coefficient very close to 1. However, if the therapy head does not have a sufficient contact surface so that waves travel through air, or if air-bubbles are present in the gel used for contact, parts of the wave may be reflected. Jain et al.[8] observed reduced efficacy of fragmentation when air-bubbles were present in the coupling medium of ESWL. This fits well with the theory mentioned above.

2.2.2 Shock Waves

A shock wave is, according to Encyclopedia Britanica, "a strong pressure wave in any elastic medium such as air, water or a solid produced by supersonic

aircraft, explosions, lightning or other phenomena that create violent changes in pressure" [38]. A shock wave often has a very high amplitude, and this causes nonlineareties in the waveform to arise. It can be characterized by an almost infinite slope up to its maximum amplitude. In a lithotriptor shockwave the rise time of the shock can be as short as a few nanoseconds.

Figure 6 shows the pressure profile of a typical lithotriptor shock wave. It features a very high amplitude peak followed by a negative pressure phase. The amplitude of this shock wave varies depending on the ESWL-generator and energy-setting. The Modulith SLX lithotriptor, a modern ESWL-generator, has a peak pressure of 105 MPa, higher than the original Dornier HM3 (the first lithotriptor on the market), which features a peak pressure of 40 MPa.

The low pressure phase of the shock wave is thought to be the trigger of cavitation. Cavitation is a fluid mechanical phenomenon where microbubbles are formed in a fluid secondary to sudden low pressure. This cavitation is an important part of stone fragmentation.
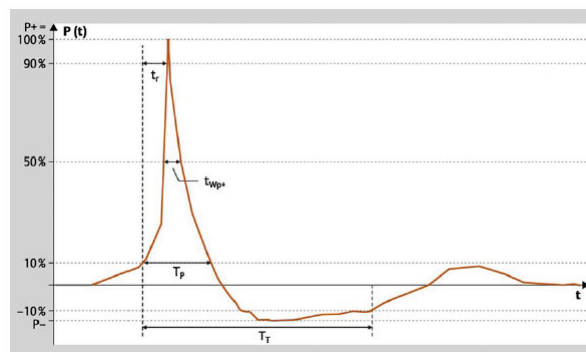

Figure 6: Pressure profile of a typical shock wave generated by a lithotriptor[34]

2.2.3   The Focal Volume of ESWL

ESWL is based on a principle were many relatively weak shockwaves are directed into the body from different directions and then intersect in a focal point. This is the point in space which receives the highest peak pressure from the wave. Around this point is something called a focal region, a region which is defined by the standardization commission IEC, as the region where peak pressure is within -6 dB of the maximum pressure (about 1/2 of the pressure). This region is usually cigar-shaped with its longest dimension in the direction of the wave. The size depends of the type of wave generation and type of machine. The pressure distribution of the focal region of a Dornier HM3 can be seen in figure 7.

Some machines have wide focus, as the low-power, wide-focus generator tested by Eisenmenger et al.[46]. Other machines have narrow, sharp focus. This characteristic may have an impact on the mechanisms of fragmentation and efficacy, further discussed below.
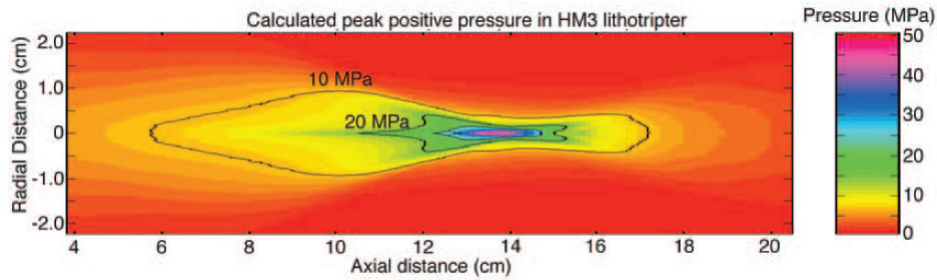

Figure 7: Pressure distribution in the focal volume of a Dornier HM3 lithotriptor, from [7]

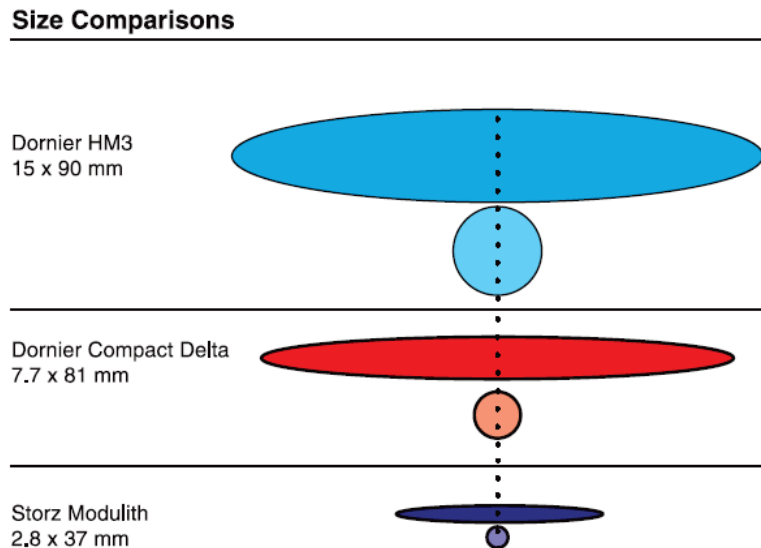Figure 8 illustrates the dimension-span in focal region of different lithotripters.

Figure 8: Comparizon of focal volume size between different lithotriptors. The dimensions are shown sideways and pointing into or out-of the image plane. Adapted from [7]

2.3 Stone Fragmentation by ESWL

Fragmentation is the separation of a material into pieces as a result of forces applied to that material. In ESWL, the calculi are subjected to forces when a shock wave hits it. The shock wave contributes to fragmentation of the stone by many mechanisms, and a lot of research have been published examining these processes. The goal of this research is to use an understanding of what processes contribute to this fragmentation to improve ESWL-equipment and treatment to achieve better results and less tissue damage.

A publication by Rassweiler et al.[34] from 2011, contains a list of theories and processes involded in fragmentation:

- Tear and Shear Forces

- Spallation

- Quasi-static Squeezing

- Dynamic Squeezing

- Dynamic Fatigue

- Cavitation

Other papers also supports this list, such as the publication from Bach el al.[9]. This section briefly describes these theories.

2.3.1 Tear and Shear Forces

Chaussy et al.[11] were among the first to describe kidney stone treatment by ESWL and they explained the fragmentation by tear and shear forces. These forces are generated as a result of the impedance difference in the stone, compared its surroundings. The sudden change in impedance cause presure gradients to arise, thereby generating tensile and shear stresses. According to Rassweiler et al. the tensile stresses are only caused when the width of the focal zone is less than the width of the stone.

2.3.2 Spallation

Spallation is, according to Sapozhnicov et al.[30], caused by the reflection and inversion of the compressive phase of the shock wave off the distal surface of the stone, causing tensile forces. These forces are highest where the reflected wave meets the tensile phase of the original shockwave.

2.3.3   Quasi-static Squeezing

Experiments conducted by Eisenmenger[17] showed cleavage parallel or perpendicular to the wave direction in experiments where the focal width were as wide as, or wider than the stone. He called the phenomenon quasi-static squeezing. When the wave passes the stone, it travels at different velocities through the stone compared to through the surrounding liquid. Waves travelling on the surface of the stone causes circumferential stress, which acts as a squeezing mechanism[34]. Eisenmenger showed this effect in his publication statically by squeezing a model stone using a clamp and observing similar cleavage as the effect caused by the shock waves.
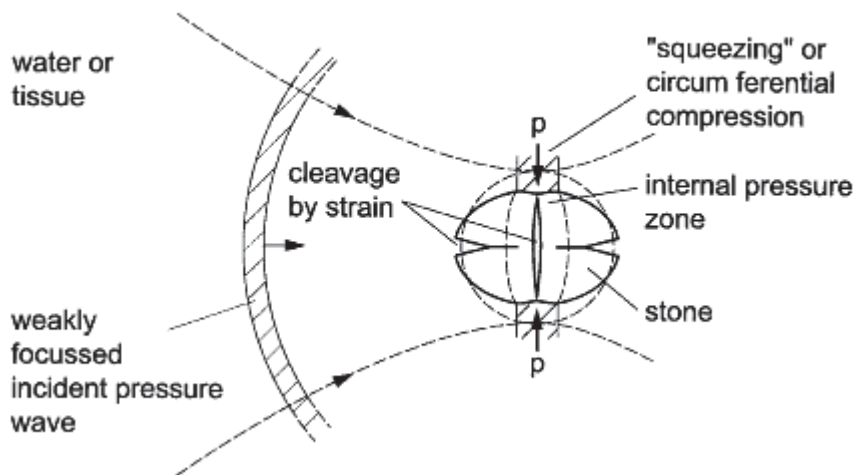
Figure 9: Illustration of the quasi-static squeezing mechanism, from [17]

2.3.4   Dynamic Squeezing

Sapozhnikov et al.[30] presents theory and experiments supporting dynamic squeezing. Fragmentation is driven by shear waves created inside the stone as a result of reflected waves from the stone-liquid boundaries. The paper presents a mathematical model used for simulating forces inside the stone when hit by a shock wave. Like quasi-static squeezing, this phenomenon requires the focal width to be at least as wide as the stone.

Figure 10 illustrates dynamic squeezing and spallation.

13
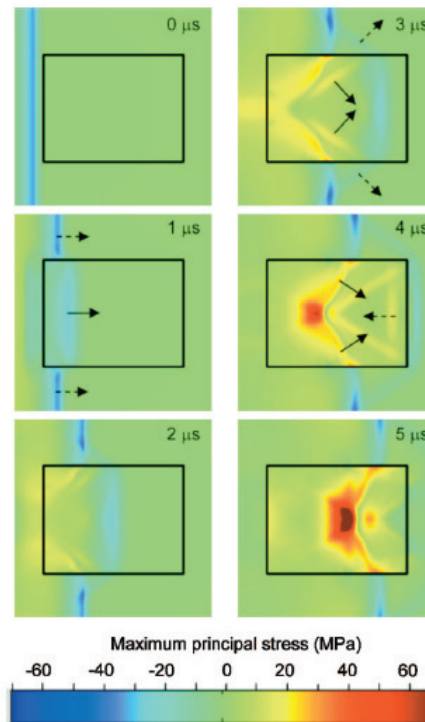
Figure 10: Simulations showing pressure inside a cylindrical stone. At $t = 4\mu s$ the reflected tensile wave cause stress when it meets the tensile phase of the shock wave, causing spallation. Even higher stress occur at $t = 5\mu s$ caused by shear stress and dynamic squeezing. From [30]

2.3.5   Cavitation

The formation of tiny vapor bubbles in a liquid, as a result of pressure changes, are known as cavitation[21]. Nuclei containing microscopical amounts of gas are required for cavitation to start. When subjected to a pressure reduction, these bubbles grow. After growing, the bubble collapses, causing local temperatures in the order 10000 $^{\circ}$K of and tiny jet streams[47].

Figure 11: Natural kidney stones treated by ESWL in vitro in water(a), and a cavitation inhibiting liquid, castor oil(b). From [39]

Coleman et al.[6] presented evidence of cavitation from ESWL in 1987. They observed that cavitation is powerful enough to puncture metal foils and deform metal plates. This led to the theory that cavitation is an important part of calculus disintegration, and 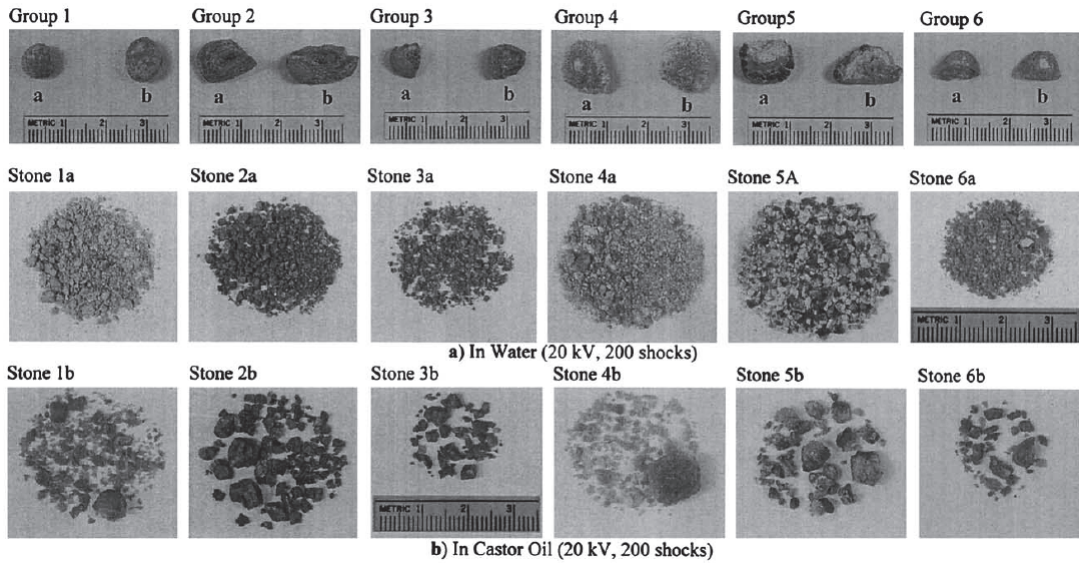many publications support this hypothesis. Cavitation may help to widen cracks as liquid enters and expand them. Cavitation also causes surface erosion and may help reduce the stone to passable fragments. Experiments done by Zhu et al.[39] show that when inhibiting cavitation by surrounding the stone in a high viscosity fluid, the precentage of passable fragments dropped from 89% to 22%. The theory presented in this article is that stress waves acount for initial fragmentation, but that cavitation is essential in reducing the smaller pieces into passable fragments.

Figure 11 from experiments conducted by Zhu et al. on natural stones in vitro, clearly suggest that cavitation plays a big role in the late stages of fragmentation. Without cavitation, large fragments still remain after the 200 shocks.

Cavitation, however, requires a liquid to be in direct contact with the calculi. Eisenmenger cites work done by Parr et al, an article not available to the author, presenting evidence of ureteral stones only fragmenting on the sides exposed to liquid.

The violent effects of cavitation also have an impact on tissue, causing blood vessels to burst and leading to hematomas. Research have been done on ESWL

under high atmospheric pressure, suggesting reduced tissue damage when using this technique[31].

2.3.6 Dynamic Fatigue

Dynamic fatigue, a theory presented by Lokhandwalla et al.[27], describes fragmentation by the development of microcracks by processes like the other ones described in this section. A mathematical model based on dynamic fatigue, also presented in the article, aims to estimate the number of shocks waves needed to break the stone into n fragments based on stone and shockwave properties.

$$N = \frac{t_c}{\tau} ln \frac{\sigma^{in}}{\sigma^{in} - \sigma_{fr}} \tag{3}$$

$$t_c = \frac{\rho c \delta_{cr}}{2\sigma_{fr}} \tag{4}$$

N is multiplied with n to find the estimated, worst case, number of shock waves required. ρ and c are the density and sound speed of the stone material. δ_{cr} is the displacement of two stone-parts needed to make microcracks coalesce (combine to a bigger crack). σ^{in} is the stress amplitude of the wave and σ_{fr} is the stress amplitude needed to form microcracks. The derivation of this model is quite complex and outside the scope of this thesis.

The authors suggest that this formula, can be used to optimize the treatment strategy to minimize damage by altering shock wave parameters as treatment progresses.

2.3.7 Summary

As presented above, many processes contribute to stone fragmentation. The can be divided into two main categories, stress waves and cativation. The fragmentation process is complicated and this section only scratches the surface of these theories, but one conclusion that may be drawn from this is that the two main categories work synergistically to fracture the stone. Stress waves are more important at the beginning of fragmentation, and cavitation is important in eroding small fragments into passable pieces.

2.4 Model Kidney Stones

When conducting research on ESWL and kidney stone fragmentation, it is important to design experiments that are realistic but also reproducible. Us-

ing real kidney stones for experiments is definately the most realistic scenario but the stones vary greatly in composition and size, which ultimately affects fragmentation behaviour. Therefore, several articles have been published presenting materials and techniques to produce model kidney stones for ESWL experiments. This section briefly presents some of the most common approaches.

2.4.1   Ultracal-30

Ultracal-30 is a gypsum cement with great surface hardness and very low expansion when setting. It is often used for creating casts or models. McAteer et al.[23] presents an analysis of model stones made from Ultracal-30 compared to the characteristics of real urinary calculi. They present results from both in vitro and in vivo experiments (using porcine kidneys), that the stone shows consistent reproducible results. The materials characcretistics are also analyzed using CT-scan and ultrasound.

To produce these stones, Ultracal-30 gypsum powder is mixed in a 1:1 ratio (g:ml) and poured into moulds. The mixing time affects the hardness of the stones, so being consistent is important. The mix is poured into moulds and left to set. When the plaster hardens, water is released, and for fragmentation testing, where stones are to be submerged in water, it is important that the stones are thourougly rehydrated if they are dried. McAteer shows that it takes approx. 96 hours for a dried stone to become rehydrated to the point where it shows the same fragmentation behaviour as a stone that was never dried.
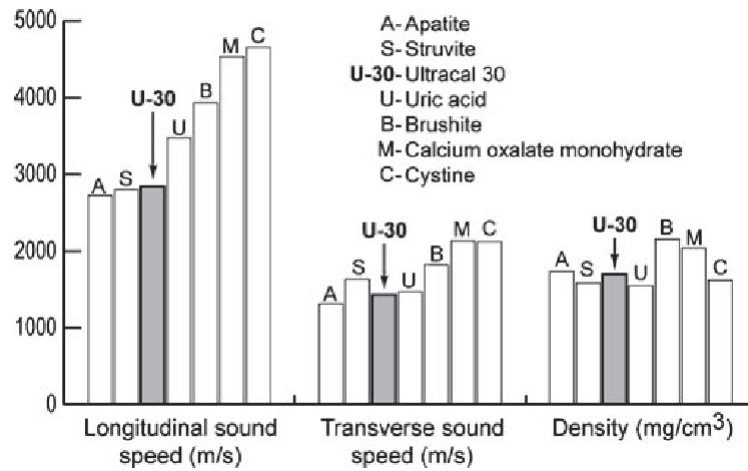
Figure 12: Physical properties for Ultracal-30 compared to natural stones, from [23]

2.4.2 BegoStone

Liu et al.[49] introduced BegoStone, a dental plaster, as a potential material for model kidney stones. By studying the physical properties, hardness and exposing model stones to lithotripter shock waves, they show that BegoStone is a useful material for experiments. This material has been adopted and is widely used [29] [48].

2.4.3 Other

Many experiments use Plaster-of-Paris as the material for model stones [39] [28] [17] [8]. This material is cheap and easy to obtain. The disadvantage of Plaster-of-Paris stones is that they tend to soften in liquid[49]. As most ESWL fragmentation experiments are conducted with submerged stones, this may cause inaccuracies if stones are hydrated for long periods of time. Therefore, many have adapted harder materials that does not show this behaviour in liquid (Ultracal-30, BegoStone).

2.5 Parameters Affecting Fragmentation

The purpose of ESWL is to fragment kidney stones into passable fragments which is defined as being 2 mm in diameter[48]. In addition, the treatment should not cause serious harm to surrounding tissue. The focal region is often much longer than the stone, and some tissue damage is difficult to avoid. A big problem is that a significant amount (more than 50%) of treatment energy miss the stone [36] [40] [44].

When choosing a treatment strategy for ESWL, many variables have to be taken into consideration. Some are device-specific, for instance focal width, which is static in most machines and cannot be changed. Others involve machine settings, such as pulse repetition rate and shock wave intensity. Various practices are used and these parameters have been shown to affect fragmentation efficacy.

2.5.1 Pulse Repetition Rate

A topic which has been subject to many studies is the optimal rate of shock wave delivery. Experiments has been made using models in a water bath, animal models, and analyzing data from real patients undergoing treatment. The conclusions are somewhat different, but they all tend to recommend a rate of 30-90 shocks per minute as opposed to 120 shocks per minute or faster.

Greenstein et al.[5] used model stones in a water bath to test rates of 30, 60, 90, 120 and 150 shocks/min with energy levels of 15, 20, and 22.5 kV at each rate. The model stones were spheres of approx 9.5 mm in diameter suspended in a sieve with holes of 2.2 mm. The experiments were stopped when all fragments had passed through the sieve. Results showed that a rate of 60 shocks/min at the high energy setting were significantly better than the higher frequncy settings, requiering only 115 shocks, compared to 273 required for a rate of 150 shocks/min at the same energy setting. They suggest that too short intervals between shock wave may have implications for cavitation, so that efficacy may be inversely proportional to the rate of delivery. The theory is that residual bubbles hinder the next round of cavitation if the interval is too short. However, no sigificant difference between rates of 60 and 30 shocks/min were observed, according to the article.

Paterson et al.[37] presents results from an animal experiment, were stones were implanted. 400 shocks were delivered to model stones at 30 and 120 shocks/min, and the percentage of mass of fragments 2 mm or greater were calculated. The fast rate, still had 81% of its mass in fragments bigger than 2 mm compared to only 45% for the slow rate. From these results they conclude

that the slow rate is more beneficial.

Studies using data from real patient treatments have also been conducted [25] [18] [24] [19]. In these studies, patients are divided randomly into groups receiving either fast or slow rates of treatment. Stone size and position are also taken into consideration. Results from these studies suggest that the optimal rate is 60 shocks/min. This rate achieves the highest fragmentation and also the least harm. The energy delivered to the body was calculated by multiplying the shock wave intensity by the number of shocks required, as a measurement of damage done, and compared to 120 shocks/min, 60 shocks/min delivered lower amounts of energy with better fragmentation.

A rate of 60 shocks/min, however, requires a longer treatment time compared to faster rates, so one study presents 90 shocks/min as the optimal rate when treatment time is also taken into consideration[26].

2.5.2 Shock Wave Intensity

It is normal treatment procedure to alter the shock wave intensity setting of the ESWL-generator as treatment progresses. According to Zhou et al.[48], two different practises are used. Going from a low setting progressively to a high setting, and vice versa. Zhou et al. also presents results from experiments done on model stones using the two different strategies. The study shows that increasing the intensity is significantly better than the other option, and it is explained with the role of different fragmentation mechanisms at different stages of treatment. Smith et al. [29] suggests that only 7.6 MPa of pressure are needed to initiate fragmentation of stones, presures that are generated even at low energy settings from stress waves. On the other hand, when the fragments become smaller, cavitation is a more important effect, and this may require higher amounts energy to produce. This is why, according to Zhou et al, the increasing energy rate is better. One could argue that a constant high energy would be better, but this would also imply more energy delivered and potentially more harm done.

2.5.3 Focal Width

Trends in lithotripter development have been pointing towards narrow focus and high energy. Eisenmenger et al.[46] presents an alternative approach, a wide-focus low-pressure lithotriptor. This lithotriptor has a focal width of 18 mm, more than twice the width of the Dornier Compact Delta. The lithotriptor was used to treat 398 stones and results showed that the average number of shocks required was less than half the number from a similar study with

a conventional narrow focus device. The treament also required less pain medication as the power setting was very low, only 9.3 kV. Another advantage of this approach is that the wide focal zone implies less need for accurate localization. Even with movement, the stone is still in focus a higher percentage of the time, compared to narrow focus generators.

The wide focus ESWL is based on the theory of fragmentation by squeezing, as presented in section 2.3, since the wave is more likely to be wider than the stone.

2.5.4   Stone Movement

Stone movement is a big problem in ESWL as it causes many shock waves to miss the stone. This motion can be as high as 50 mm[15]. Cleveland et al.[15] presents results form an in vitro experiments showing that fragmented mass percentage dropped from 75% to 50% when treating a stone moving +- 10 mm compared ot a stationary stone. Fragmentation further dropped when movement was increased. These results were also consistent through different energy levels and rates. Figure 13 shows stones from these experiments.
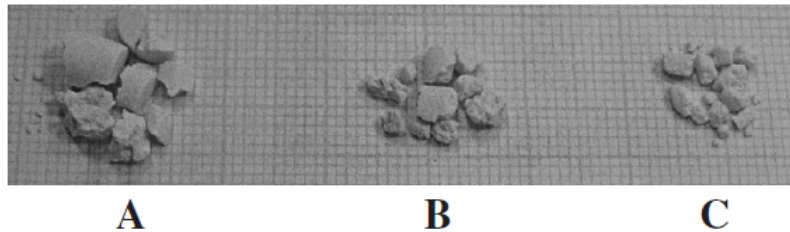

Figure 13: Stones treated with 400 shock waves with (A): ±25 mm of motion, (B): ±5 mm of motion, (C): No motion. Figure from [15]

The authors propose two possible solutions to the problem of movement. Jet-ventilation, a way of ventilating a patient under anasthesia with minimal movement, or stone tracking. With stone tracking, shots are only fired when the stone is estimated to be in focus, and thus the stone receives most of the energy, minimizing tissue damage. The procedure can be done in the same amount of time, or even less, as the total number of shocks will be decreased and misses eliminated.

Smith et al.[29] found a correlation between average peak pressure on a stone during an experiment, and fragmentation, which is consistent with the above statement that more hits lead to better fragmentation.

2.6 Tissue Damage

According to Chaussy et al.[14], processes contributing to stone fragmentation may also contribute to tissue damage. They list two main effects: Cavitation and tissue-air interfaces.

Cavitation may occur in the collecting systems of the kidney causing bleeding. Cavitation bubbles may also block the shock wave causing it to loose energy and damage to occur where the bubbles collapse. This may cause tissue damage as well as impair the fragmentation process.

Another possible effect may happpen if the shockwaves encounters gas-filled organs such as lungs or bowels. This transition wil cause the wave to reverse and tensile forces to appear because of the change in acoustic impedance between the two substances, (see figure 5). This can cause organs to rupture.

3   Effective Frag. with the Dornier Lithotriptor

The lithotripter used for tests in this thesis is the Dornier Compact Delta. It is a modern ESWL-generator with a narrow focus, the focal region measures 7.7 by 81 mm (see figure 8). It features energy levels from 12 - 20 kV and shock wave rates of 60 to 120 shocks per minute.

As the focal zone is quite narrow, the domimant processes in fragmentation, according to theory, is tear and shear forces, spalling and cavitation. Processes like squeezing require the stone to fit inside the focal zone, but this may still hold for small stones. A rate of 60-90 shocks/min is optimal, according to the studies presented.

As mentioned in the previous section, a problem with ESWL is the number of missed shots. This is especially the case with a narrow focus generator, as the target zone is smaller than with a wide focus. To improve the efficiency of fragmentation, and to minimize damage to surrounding tissue, it is desireable that the percentage of fired shots that hit the stone is as high as possible.

Several approaches have been used in research to increase hit percentage. Special belts have been tested, used to compress the abdomen and minimize kidney movement [34]. 'Jet Ventilation' is another teqnique that has been tested, where the patient is under general anasthesia and ventilated with minimal lung movement[16]. A third approach is to utilize ultrasound imaging and object tracking in images to track the stone in order to fire shots only when the stone is in focus. This approach have been presented in several papers [12][13][22][32][33], and is the focus for the on-going project this master thesis is a part of. The previous work done in this project is described in section 1.2.

Figure 14 shows a screenshot from the tracking software originally developed by Tøraasen[44].
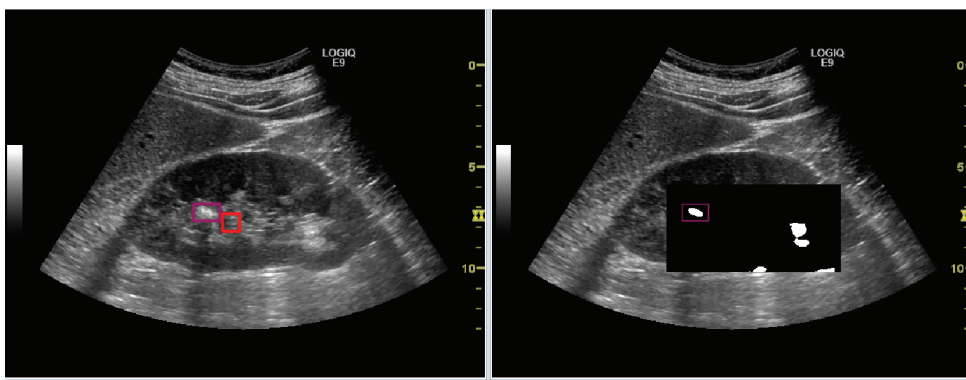

Figure 14: Kidney stone-tracking in ultrasound image, from [44]

Even when using tracking, some parameters still have to be taken into account to maximize the efficiency of fragmentation. One important parameter is where to place the focus of the lithotriptor. If the stone movement is assumed to follow a sinusoidial movement, the time the stone spends in focus will vary greatly depending on where in this trajectory focus is placed. The most optimal would be to place the focal region where the trajectory of the stone turns, as this would make the stone spend the longest time in the focal zone. It may be hard to find the optimal point of aim, but the closer the aim is to the turning point, the lower the assumed speed of the stone is, and thus more time available for hits each cycle.

If it is assumed that the tracking will enable every shot to hit the stone, the question is what strategy will produce the most eccifient fragmentation, such as energy setting and rate. A normal treatment strategy is to gradually ramp up the shock wave energy to induce some protective effects in the kidney[14], and this strategy is fully compatible with using tracking. A system enabling shots to hit every time, may also enable the increase in energy to be steeper.

Several studies have shown that pulse repetition frequency affects fragmentation, see section 2.5.1, and this will have to be taken into consideration when using tracking. While shock waves may not be fired at a constant frequency when using this system, an upper bound on the firing frequency should be used to ensure that the frequency do not get too high. According to the reseach presented, the problem is using a too high frequency, so a frequency lower than the recommended 60-90 shots per minute should not cause a decline in effectiveness.

4   Full Test Setup Description

To evaluate the performance of the tracking system, a test setup is needed. Since the tracking software utilizes prediction, the delays of the test setup modules must also be known. This section presents a description of all the main system modules in the proposed full test setup, their purpose, the interfaces between them, and the delays involved. The system can be viewed as a chain of information flowing in a clockwise direction, see figure 15. An image of the stones position flows from the ultrasound scanner to the PC, which sends a trigger signal to a control unit. The control unit sends a signal to the lithotriptor, which ultimately delivers the treatment to the kidney tank (the "patient"). Computations and data transfers introduces the delay into this chain.
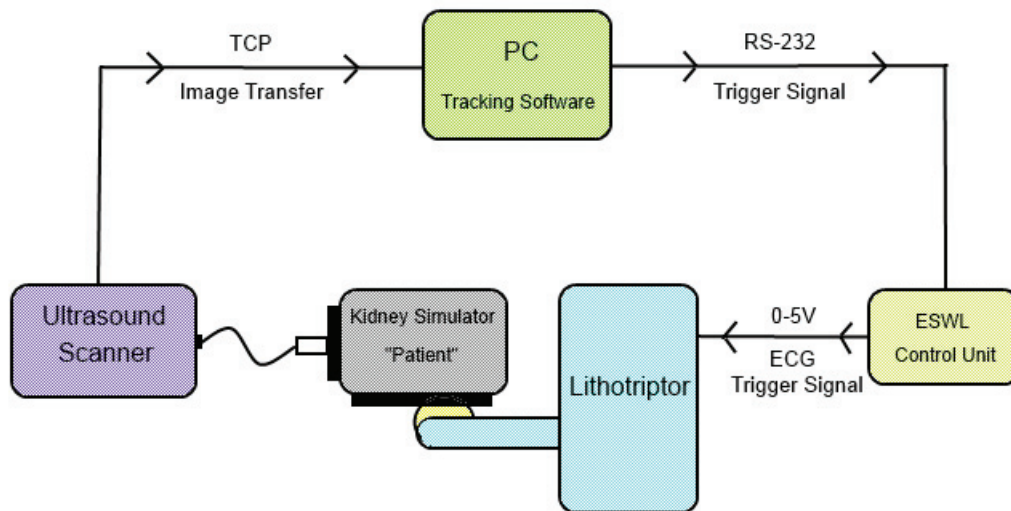
Figure 15: Modules of the full system and their interfaces

4.1   Kidney Simulator Tank

The kidney simulator tank contains the model kidney stone, submerged in water. A servo motor can generate stone movement in one dimension. The tank has two flexible plastic walls mimicking skin and tissue, one on the bottom and one on the side. The bottom wall serves as the contact point for the litotriptors water-filled cushion, where the shock waves are transferred through.

The other wall provides a surface for the ultrasound probe to scan the tank. The purpose of the tank is to create an environment where stone movements can be controlled. Realistic movements can be created using the servo, and the stone can be fragmented by the lithotriptor, like in a real treatment setting.

4.2 Ultrasound Scanner

The ultrasund scanners probe is placed on the surface of one of the flexible walls of the kidney simulator, to scan the simulator tank. The purpose is to produce a stream of images where the stone is visible, to be able to track its position. This means that the scanning plane of the probe should be approximately equal to the movement plane. The ultrasound scanner runs a server that the PC can connect to, to receive the stream of images. The stream is transferred over an Ethernet connection, using TCP, over an interface called Ulterius. The system does not feature synchronization of the focal point between ultrasound equipment and lithotriptor. For testing in a controlled environment, like this one, the stone may be placed in the focal point using x-ray and then the point can be defined in the ultrasound images, and thus eliminating the need for synchronization. This requires the probe to be fastened and not move in relation to the lithotriptor during treatment.

The time from an event occuring (stone movement) to the PC receiving an image of that event is be the delay of this module. It can be split into three main parts: The ultrasound sweep, the post processing of image data, and the image transfer.

4.3 PC with Tracking Software

The PC is the main control unit of the full system. It runs a tracking program which controls the system functions. The tracking program connects to the ultrasound scanners server and streams real-time images from the kidney simulator. For each new image received, a tracking algorithm is used to identify the stone. An estimation of position, based on the stones previous movement pattern is then used to predict the stones future position. This is done because of the delay introduced in all parts of the system chain. As the triggering module also adds delay to the chain, a trigger signal must be sent out at some time before the stone is estimated to be in focus. The signal to trigger the lithotriptor is sent to the ESWL control unit using a RS-232 interface. The PC-module itself also adds delay to the system, carrying out the steps: Receiving and constructing ultrasound image, tracking and prediction, output of trigger signal.

4.4   ESWL Control Unit

The ESWL Control Unit is a circuit board containing an MCU with a RS-232 interface and digital ouputs. As soon as a trigger request is received from the computer, it puts out a trigger signal to the lithotriptor in the form of a short 0-5-0V pulse. The signal replicates a trigger signal sent from an ECG monitor which can be used to trigger shock waves. The delay of this module is negligible as it involves minimal data transfer and no computation (see section 7.1.1).

4.5   Lithotriptor

The lithotriptor is ultimately responsible for delivering the treatment energy to the patient, disintegrating the stone. It sends shock waves through a cushion to its focal point, inside the kidney simulator tank. This is the point where the stone must be to receive the full energy if the shock wave. The lithotripter is triggered by a ECG signal sent from the ESWL control unit. The time it takes from receiving the signal, until firing a shock wave is the triggering delay. The propagation time of the shock wave from the generator to the stone is the last delay of the chain, but this is assumed to be negligible because of the high sound speed in water.

4.6   Summary of Delays

The biggest delays will affect the system performance the most, and these can be summarized in the following bulletpoints:

- Ultrasound scanning and processing time

- Image transfer time from ultrasound scanner to PC

- Tracking algorithm processing

- Lithotripter triggering delay

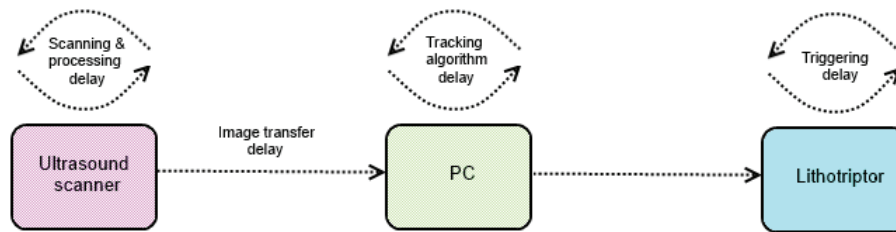Figure 16 presents a simplified figure of the systems showing the main delays.

Figure 16: The main delays of the full system

5 Design of System Modules

Some of the modules in the test system had been obtained or developed in previous work. A summary of these existing modules are:

- Tracking program

- Ultrasound scanner and image transfer system (Gained access to by SIN-TEF)

- Kidney simulator tank

New modules of the test system were obtained and designed for this thesis to be able to create a complete test setup. These were:

- Lithotriptor (Gained access to by St. Olavs Hospital)

- ESWL control unit

- Kidney simulator tank (improved over previous design)

- Model kidney stones

The lithotriptor at St. Olavs Hospital is normally operated using a fixed pulse repetition frequency. To enable the control system to release individual shock waves, another approach was needed. A trigger system was therefore developed. Other parts of the exixting test equipment was also improved and added to. The kidney simulator tank was improved and the movement system were made more accurate, but still keeping the same components. In addition, phantom kidney stones were moulded from a special gypsum for use in fragmentation tests.

5.1 ESWL Control Unit

Controlling the lithotriptor had not been done in any of the theses preceding this one, so a control unit had to be developed. Two designs for this control unit are presented here.

During treatment, the lithotriptor is controlled via a hand-held control, connected by a cable. A big button on the control is used to initiate the firing of shocks. In the first design of the control unit, an extension cable for the remote was made to be able to control this button-press. This design was abandoned when a better interface was found. The lithotriptor has an option to control it via an ECG monitor to enable shock waves to be triggered by patient heartbeats. A control unit using this interface was developed and tested.
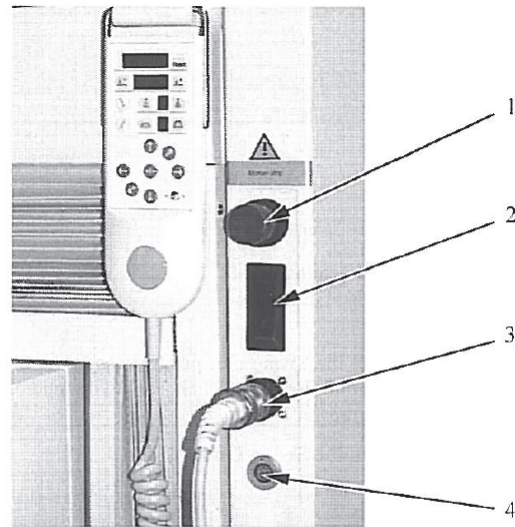
1   Motion-stop switch
2   Main switch
3   Connection for hand-held control
4   Connection for localization arm

Figure 17: The hand-held control for the Dornier Compact Delta, from [2]

5.1.1   Controlled Button-press

The big, round button on the hand-held control is used to initiate shock wave release. During treatment this button is held pressed. Connecting this button to a computer via a relay to be able to fire a single shot was the idea for the first ESWL-control unit.

Figure 17 shows the hand-held control and its connection. The biggest button on the control is used to activate the shock waves. From the service manual it was found that when the button is pressed, four wires in the cable are connected, two and two together[3]. To control this function from a computer, an extension cable was made, with a custom designed circuit board connected. This circuit contained a two-pole relay connected to the same wires as the button controlled. The relay board was connected to an Arduino board to enable one of its digital outputs to control the relay. The controller cards connected to the extension cable and the connectors used is shown in figure 18. The connectors used were Amphenol ECTA 133 series. This is the same standard as the lithotriptor uses, and could therefore be connected directly to the machine and remote cable.
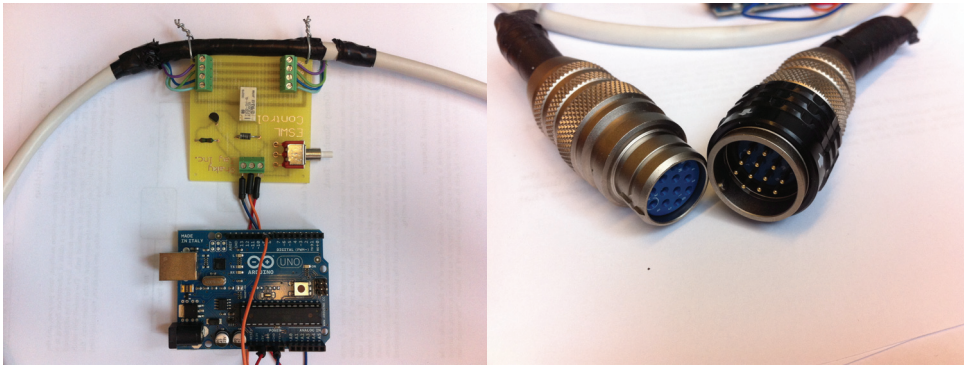
Figure 18: The button-press controller card(left) and connectors(right)

This controller unit was tested in the Dornier Compact Delta at St. Olavs Hospital and was found to work for triggering shock waves in the same way as the button on the hand-held controller.

A big disadvantage with this approach was the possibility for unpredictable delays. The button mechanism is used for initiating treatment and must be held pressed for shock waves to be released. No documentation was found explaining if a shock would be released immediately after a press or what delays would occur. Therefore, after identifying the ECG-trigger option, this controller was abandoned.

5.1.2 Replicated ECG-signal

The Dornier Compact Delta features an option to synchronize shock wave release with the patients heat rate. The second ESWL control unit design utilized this interface to the triggering mechanism. A triggering module can be added via a BNC interface on the lithotriptor. The control circuitry inside the lithotriptor, shown in figure 19 features galvanic isolation using an opto-coupler, so the interface was also safe to use.
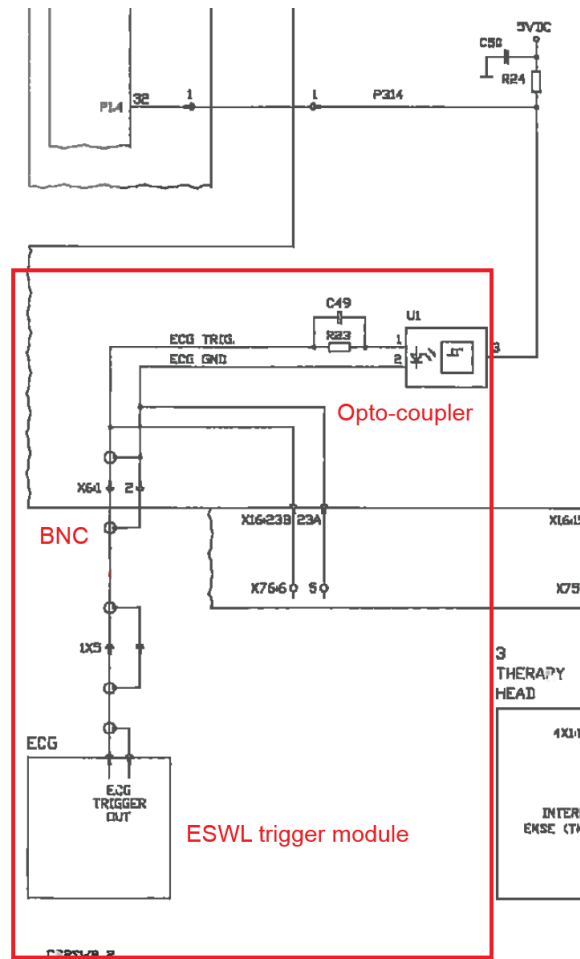
Figure 19: The ECG-control circuit in the Dornier Compact Delta, from [4]

From the service manual it was found that the control signal used for this interface, was a simple 1 ms square pulse of 0 to 5-24 V, and this corresponded well with the digital outputs of the Arduino, which puts out 5 V for a digital '1'. As the lithotriptor is an expensive piece of equipment, and the only one in the hospitals posession, it was important make sure the circuit would not be overloaded with current. The manual did not describe the value of the resistor in the ECG-circuit, so this was measured with the lithotriptor powered off and with a voltage of only 2,5 V. It was found to be approx 700 Ohms and the desicion was made that it was safe to send the 5 V from the Arduino straight into the machine. The triggering was verified to work in a test at St. Olavs Hospital.
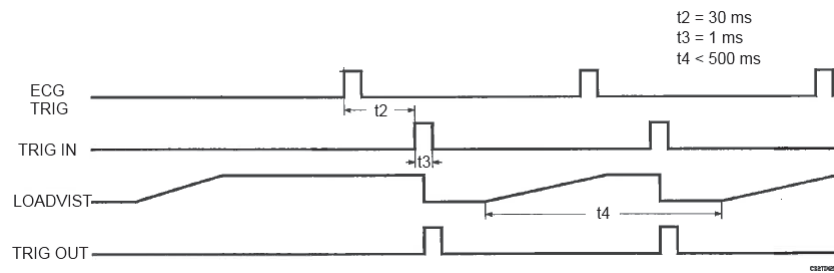
Figure 20: Timing diagram for ECG-triggering, from [4]

The advantage of using the ECG-trigger was that documentation showing the timing for the triggering process was available. Figure 20 shows the timing diagram, where the signal "ECG TRIG" is the signal generated by the Arduino. The signal "LOADVIST" is the voltage of the energy storage circuit and the sudden drop of the signal indicates the release of a shock wave. If the real system follows the timing diagram, a constant delay of between 30 and 31 ms is expected between sending the signal from the control unit and a shock wave being released. The diagram also shows that 500 ms is the minimum time between releases, giving a maximum pulse repetition frequency of 120 shocks/min when using this triggering mechanism. The finished trigger module is shown in figure 21. A plastic cover was added to the Arduino for protection.

Figure 21: The ECG control unit with BNC interface

5.2   Kidney Simulator Tank

Runnestø designed and built a kidney simulator tank for his project thesis[35]. This was also used in the authors project thesis[40]. Figure 22 shows the old design.
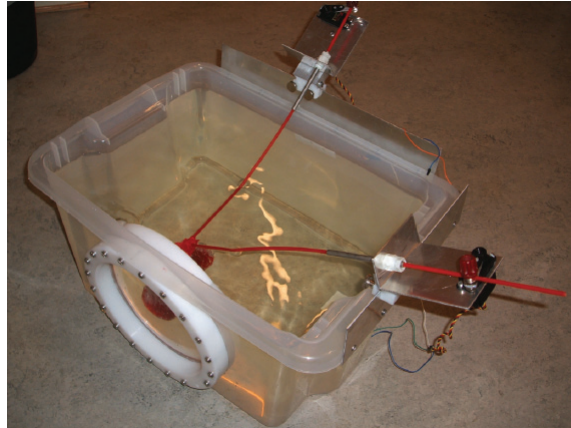
Figure 22: The old kidney simulator tank designed by Runnestø for his project thesis[35]. Picture taken from his thesis.

For the tests done in this thesis however, this tank was found to be inadequate. The shock waves are delivered from below and thus another flexible wall in the bottom of the tank was needed. A new, more compact tank was designed, with two flexible walls, see figure 23. The two flexible walls makes the tank compatible with both the lithotriptor and the ultrasound scanner at the same time, which is essential if the full system is to be tested. The new tank was built was built by the workshop at the Departement of Engineering Cybernetics at NTNU.

The movement system was also improved. The original system featured two servos, generating three-dimensional movement, connected to the phantom using flexible plastic rods. While this setup were able to generate complex movement patterns, it was also very difficult to predict what movement was generated for different servo inputs. To do repeatable tests, more control was needed over the phantom movement. The old system was therefore altered to allow a more precise one-dimensional motion.

To place a stone in the focus of the lithotripter, an x-ray system is used. Images are taken in two angles, one directly above the patient, and another in a 30 degree angle from the vertical scan. It was therefore important to be able to ajust the phantoms position in one plane at a time. The ajustable fastening mechanism in the bottom of figure 23 was added for easier focusing.
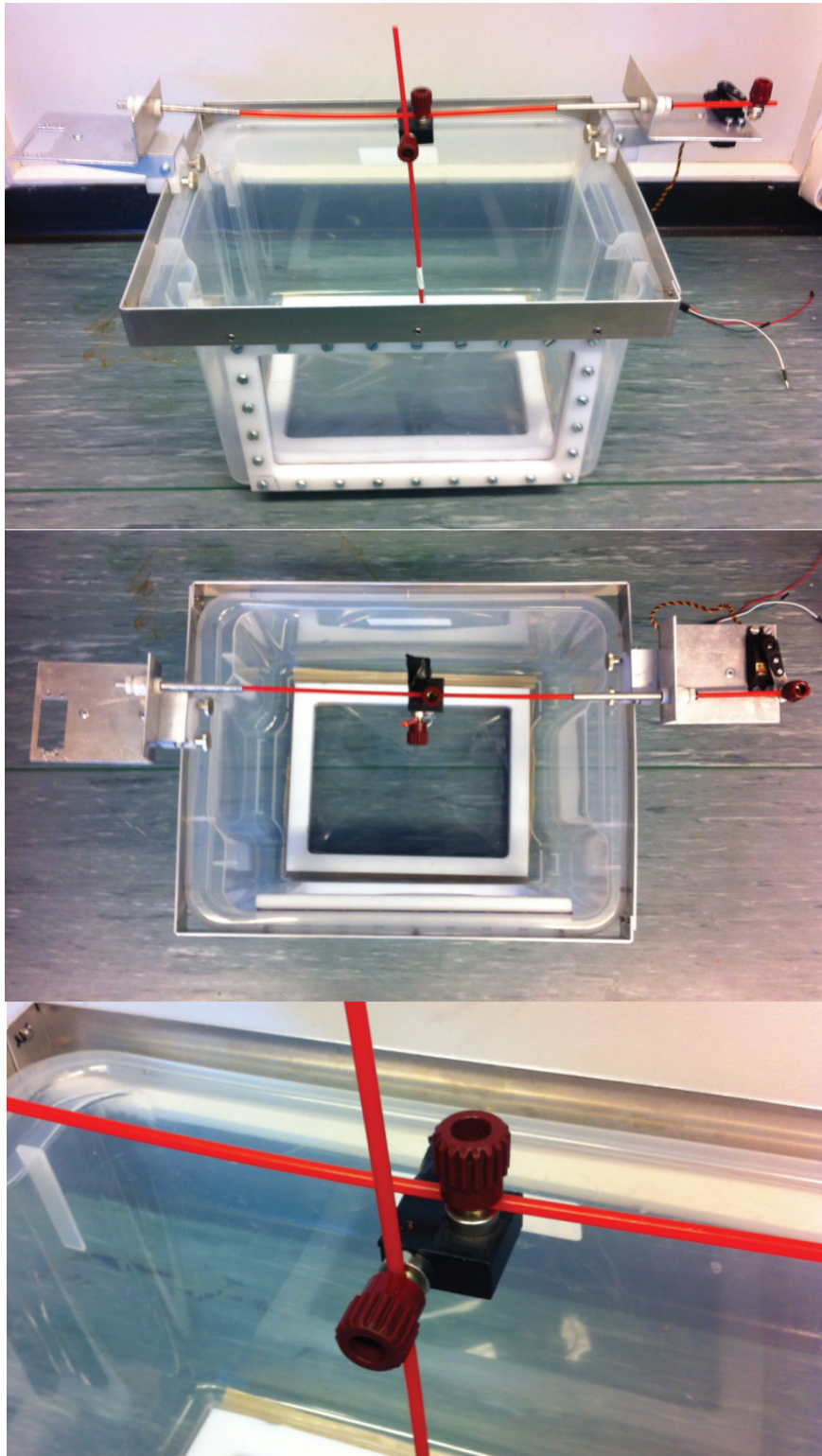
Figure 23: The new kidney simulator designed for this thesis.

To hold the model stone and contain the fragments of the stone during treatment, water-filled plastic glove-fingers, closed by plastic strips, were used. A holding mechanism was made from steel wire. The containers and holding mechanism can be seen in figure 24.
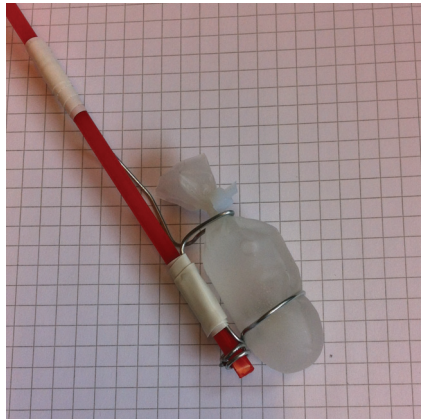

Figure 24: Model stone container and holding mechanism

5.3 Model Kidney Stones

Ultracal-30 was chosen as the material for model kidney stones as they are widely used in research. Ultracal-30 powder was mixed with tap water using a ratio of 1:1 (g:ml) as presented by to McAteer et al. [23].

The slurry was mixed in a drink shaker for 5 minutes, and then transferred to a mould. Each well in the mould was filled to the top using a syringe and then left to dry for 1 hour. After this, the mould was submerged in water and set to dry for 24 hours. The stones were then removed from the mould and put into a small, water-filled container. McAteer et al observed that stones dissolved faster when stored in larger volumes of water. They also showed a correlation between fragility and storage time in water, stones stored longer were more fragile. Because of this, the time from manufacturing and doing experiments with the stones using ESWL, were kept approximately constant for all the experinemts. The time used from removing the stones from the mould until the experiments were approximately 5-10 hours. Figure 25 shows the finished stones.
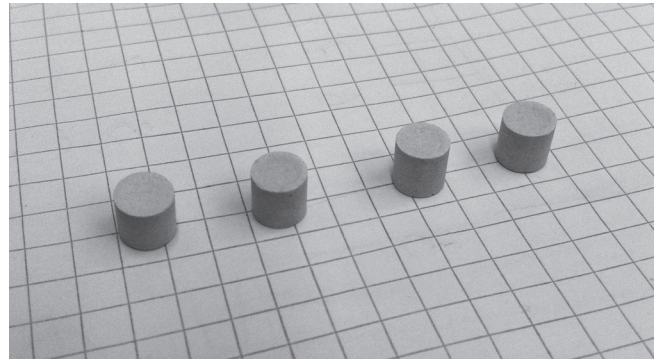
Figure 25: Ultracal-30 phantom kidney stones (Grid: 5 mm)

The mould was made of plastic, consisting of two rows of 10 wells, where each row consisted of two plastic parts held together with screws. This was done to allow easy extraction of the stones after drying. Each well measured 6 mm in diameter and 8 mm in height, and produced stones of 6 mm in diameter and 5,5 mm high. The mould was manufactured in the workshop of the Department of Engineering Cybernetics at NTNU, it can be seen in figure 26.
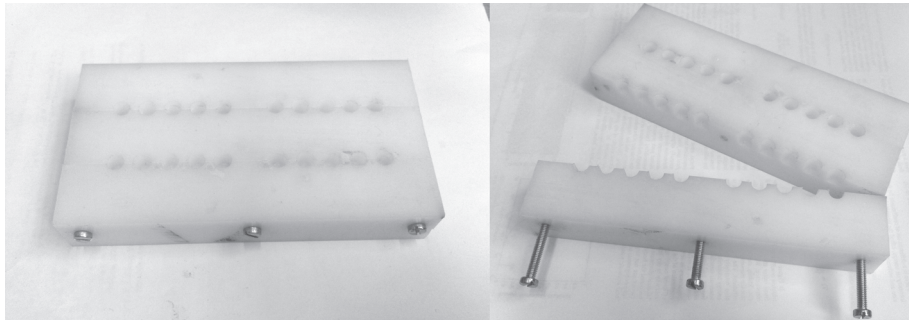
Figure 26: The mould used for phantom stone casting

6 Test Desctiptions

For this thesis, two categories of tests were performed; Test setup module tests and fragmentation tests.

The tests of individual system modules are important both to verify the modules functionality and to determine the delays associated with each module. As mentioned above, the system is dependent on prediction to function, and therefore, a known delay is needed. This delay is highly dependent on the individual components of each module, and must be tested for all new and modified modules. The modules tested here are the imaging and tracking system and the triggering module. The reason for doing a combined test of imaging and tracking system was that the image transfer protocol in the system is based on a proprietary API, and it is therefore not possible to run tests on the ultrasound equipment only.

The second category of tests, fragmentation tests were done to examine the difference in fragmentation between moving stones and stationary ones, as well as examining the difference between model and real stones. Tests with a moving stone were done to simulate a real treatment condition, while a stationary stone, where all the shockwaves hit, were a way of simulating treatment under the assumption that a tracking system enabled all the shock waves to hit.

6.1 Delay Test for Imaging Module and Tracking

The delay test done in the authors project thesis[40] was repeated for this thesis since a new test computer was used. The test setup is shown in figure 27.
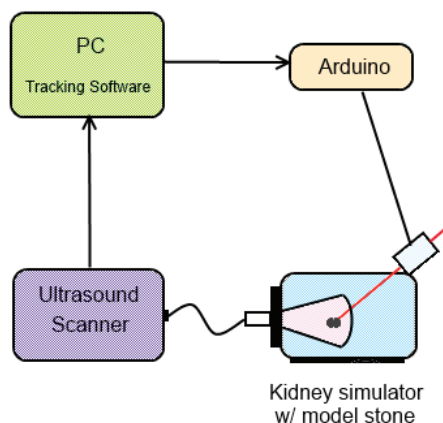
Figure 27: The test setup for the image system delay tests

To measure the delay of the imaging and tracking part of the system, the time was measured from when a model stone movement was generated in the kidney simulator tank, until the tracking software registered movement. The ultrasound scanners probe was placed on on of the tanks flexible walls to enable it to capture images of the stone. Because of the limited scan depth of the probe (9 cm), the model stone had to be placed as near the inside of the flexible wall as possible. The tracking software with the image transfer extension developed in the authors last thesis was run on the test PC. An Arduino was used to control the model stones movement in the tank. An extension to the tracking program enabled a small "jerk" movement of the servo to be generated.

The tracking program measured the time from after sending the signal through RS-232 to the arduino, until the tracked object (the stone) moved two pixels. The threshold of 2 pixels was the smallest displacement that ensured that the system was not triggered by small movements or inaccuracies in the image. The procedure was repeated a number of times for three different framerate settings on the ultrasound scanner, 14 fps, 11 fps, and 8 fps. The tracking program also logged the trakcing loop time for each frame.

Table 28 summarizes the test PC specifications.

Manufacturer	Toshiba
Model	Satellite
Operating System	Windows XP
CPU	Intel Core 2 T5500 1.66 GHz
Memory	1,5 GB

Figure 28: Test PC specifications

6.2 Delay Tests for ESWL Triggering System

A delay test for the triggering system was conducted to verify the timing diagrams in the service manual of the lithotriptor (see figure 20).

To measure this delay, an oscilloscope was connected to the triggering output, to visualize the trigering signal. A microphone was placed on the patient table, close to the kidney simulator tank, to pick up the sound emitted when a shock wave was released. The microphone was connected to another channel of the oscilloscope through an amplifier. The ECG-trigger was programmed to fire at a fixed frequency, and images from the oscilloscope showing the time difference between the two events were stored. Figure 29 shows the test setup.
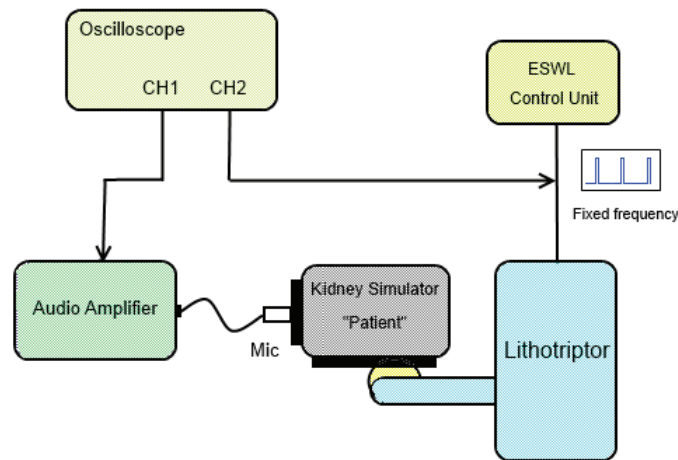
Figure 29: The test setup for the lithotripter trigger delay test

6.3 Fragmentation Tests

To investigate the difference in fragmentation efficiency between a stationary and a moving stone, fragmentation tests were performed. Testing the kidney simulator combined with the lithotriptor was also useful to verify their compatibility. To simulate a moving stone, a respiration pattern was implemented on the Arduino. Section 6.3.1 presents the movement pattern and implication for aiming at different parts of the oscillation, and section 6.3.2 describes the test setup in more detail.

A test to compare fragmentation result between a model- and real stone were also performed.

6.3.1 Movement Pattern

Since the movement of kidney stone inside the body is mainly respiratory induced, the stones were assumed to follow sinusoidal trajectories. Normal breathing rate is between 14-18 respirations per minute for adults. Based on this, the period chosen was 4,3 seconds, corresponding to 14 breathing cycles per minute. The total lateral movement of the stone was chosen to be 50 mm, based on experiments by Cleveland et al.[15], meaning an amplitude of 25 mm. A simple Matlab script was used to pre-calculate the degree outputs to the servo and this was stored in a lookup table on the microcontroller to ensure predictable runtime during testing. The movement program source code can be seen in appendix B.
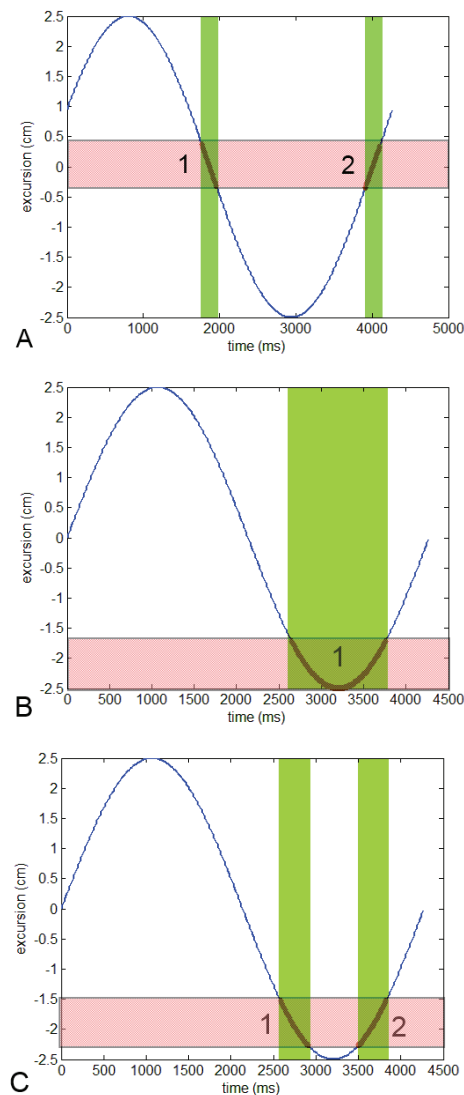
Figure 30: The graph shows the movement of the **center** of the stone in x-direction per milliseconds. The red color marks the focal zone and the green bars indicate the regions where the stone is in focus.

Figure 30 shows the **center** of the stones movement when a respiration rate of 14 resp/min and an excursion of 50 mm is used. Placing focus in the middle of the oscillation, as in case (A), is the least optimal, as the stones velocity is highest in this region. The stone only spends 210 ms inside the focal region for each pass. The most optimal is placing focus over the top or bottom of the graph, as in case (B), where the stone turns. In this case, it will result in a timespan of 1097 where the stone is in focus. However, it may be difficult to

place the stone exactly in this region, without overshooting. A more realistic focal placement is shown in the figure on the bottom (C). Here, the stones velocity is much lower in the focal zone compared to a center focus, and thus the stone spends more time in the focal zone per breathing cycle, 336 ms per pass.

6.3.2 Test Setup

For this test, the lithotriptor was run in normal treatment mode, using a fixed frequency of 90 shocks per minute and energy level 3. Each stone were subjected to 600 shocks.

For the stationary tests, the stones were placed in the focal point using x-ray localization. For the movement tests, the stone was first placed in the focal point with the servo arm in a fixed position to enable focus to be similar to case "C" in figure 30. Movement was then enabled and the stone was confirmed to pass through the focal point using x-ray localization.
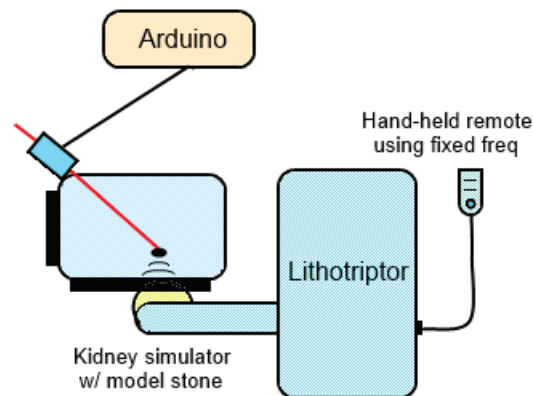
Figure 31: Test setup for the fragmentation test

Figure 32 shows two photos taken during testing. The tank had to be placed in an angle so that the treatment arm did not block the x-rays. To locate and place the stone in focus, x-ray images were first taken directly from above and the stones position was ajusted using the the ajustable rod mounts. To place the stone in the right height, a 30 degree image was also taken, by tilting the x-ray arm. After the stones porision was verified in both image planes, treatment was commenced.
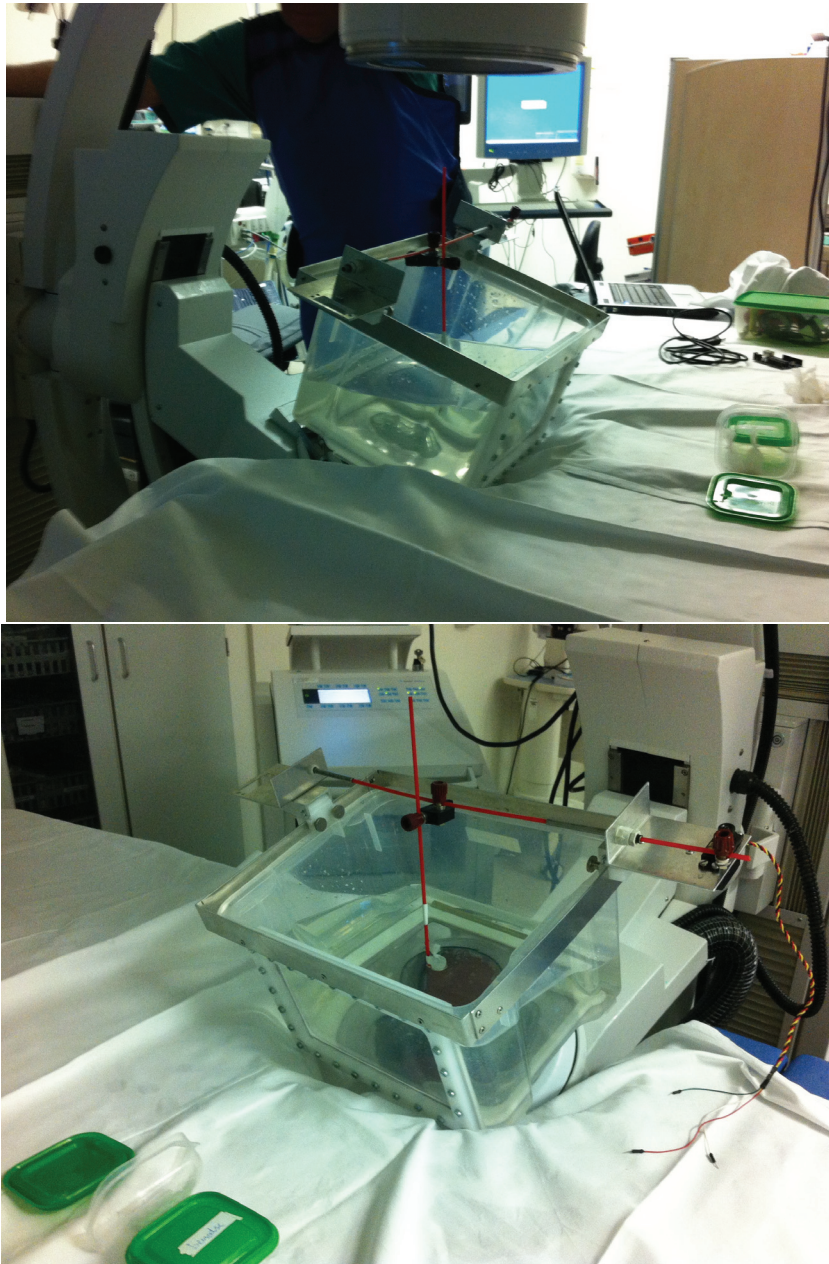
Figure 32: Photos taken during the fragmentation test

Figure 33 shows the x-ray image taken from above. In this image, the stone is barely visible, located in the middle of the mouting mechanism.
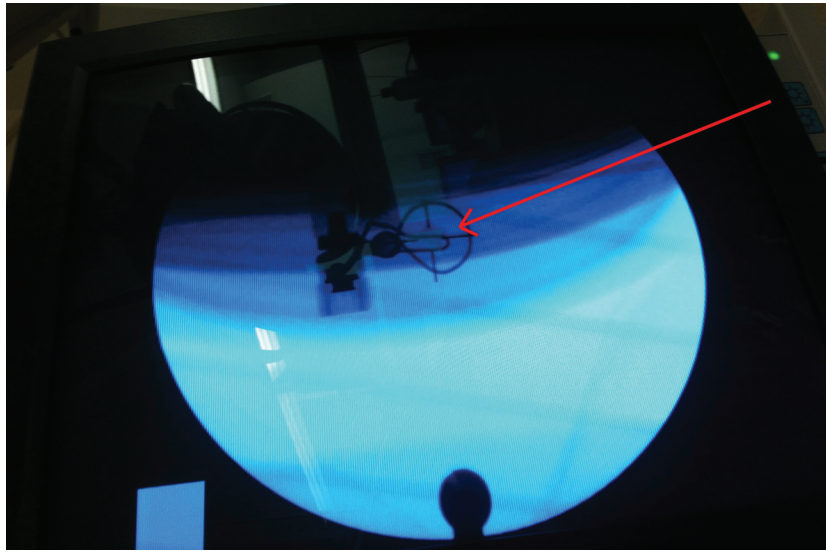
Figure 33: The stone and mounting mechanism seen on the x-ray monitor. The model stone is in the middle of the crosshairs, marked by the red arrow.

7   Test Results

This section presents the results from the tests performed. First, the results from the delay tests are presented, both in number format, and graphically. After this, results showing the delay of the ESWL-control unit are presented. The last part presents results from the fragmentation tests.

7.1   Delay Test for Imaging System

A number of samples were taken for each of the three framerates and some statistical values were calculated, shown in table 1. The best average delay occured when using 14 fps, but this also had the highest standard deviation. Only 11 ms separated the mean delay of 11 and 14 fps with 11 fps having the lowest standard deviation. Some spikes in delay occured during the testing. For 14 fps the highest spike was 736 ms. The highest spike of 11 fps was 400 ms, only 110 above the average. The lower bound on delay was approximately equal for all the different framerates, a delay of approx 170 ms. The standard deviation was calculated with the built in function in OpenOffice Calc.

Framerate	14 fps	11 fps	8 fps
Number of samples	225	206	207
Average delay	279 ms	290 ms	322 ms
Standard deviation	76 ms	46 ms	55 ms
Max value	736 ms	400 ms	455 ms
Min value	170 ms	177 ms	170 ms

Table 1: Delays of the total imaging and tracking system

The tracking software logs the time used by the tracking algorithm for each image received. These delays are shown in table 2. The reason for the high number of samples compared to table 1, is that this time is measured for each frame received.

Framerate	14 fps	11 fps	8 fps
Number of samples	5094	4730	4335
Average tracking loop delay	20 ms	20 ms	17 ms
Standard deviation	5 ms	4 ms	1 ms
Max value	34 ms	31 ms	30 ms
Min value	8 ms	8 ms	8 ms

Table 2: Delays of the tracking loop only

Figure 34 shows the distribution of the total delay for the different framerates. The height of the individual bars indicate the fraction of the samples at that delay value.
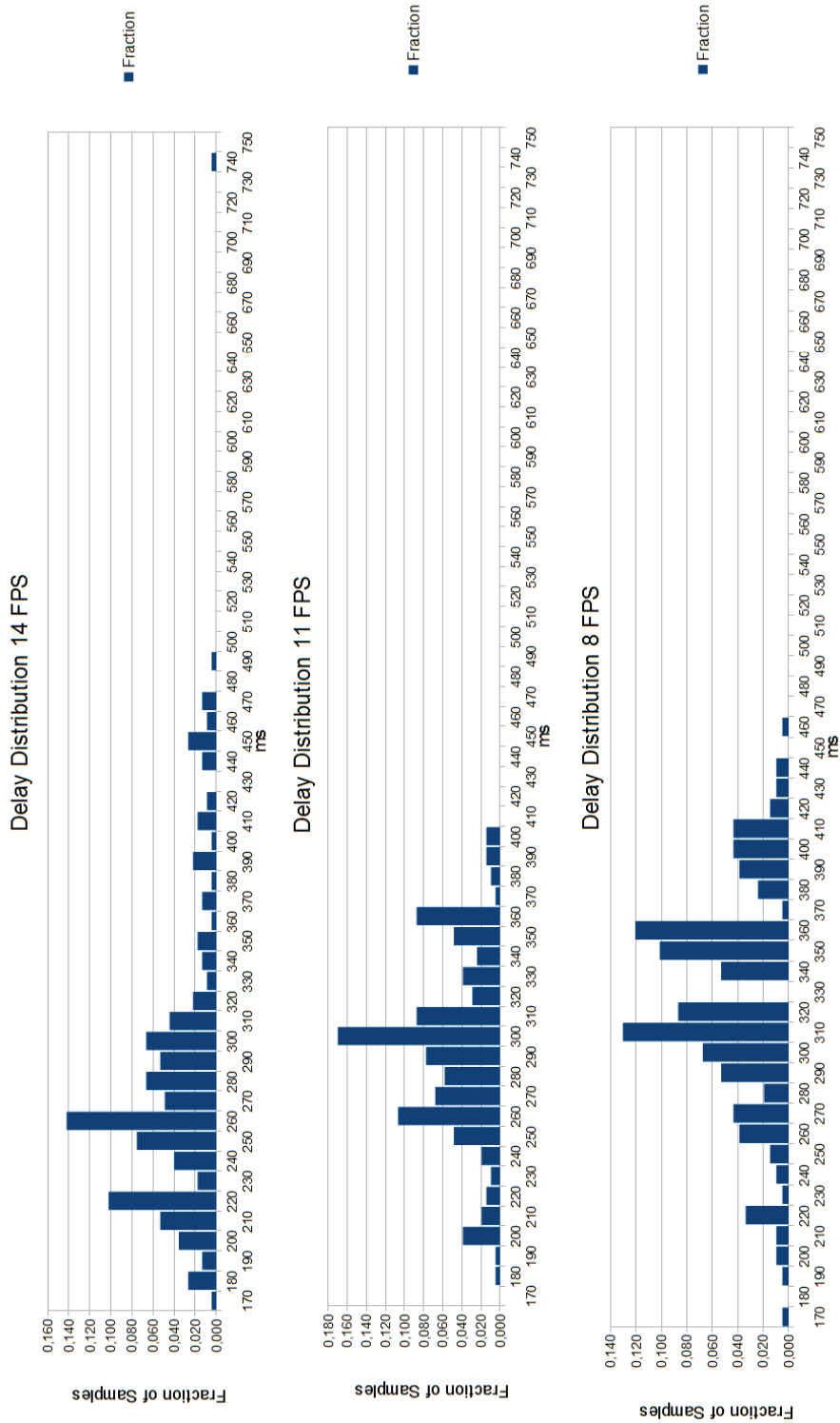
Figure 34: Delay distribution in ms for the imaging delay tests

7.1.1 Possible Sources of Error

The purpose of this test was to measure the delay from an event occuring in the tank, to that event being registered in the tracking software. Since the time was measured from after sending the signal over serial, a possible source of error in this measurement is the time it takes for the arduino to control the servo to its new position. The servo is controlled using pulse width modulation (PWM), meaning that the angle is controlled by sending a 20 ms pulse of high an low voltage where the fraction of high voltage in the pulse determines the angle. This requires the control signal to be updated 50 times per second. The worst case delay will occur if the Arduino receives a signal to change the angle right after a pulse has been initiated. This case would imply an approx. 20 ms delay for moving the servo. The real delay was measured using a high-speed camera filming the Rx-led on the arduino and the servo arm. The Rx led lights up when the servo receives serial data, and the time was measured from after the last byte was received until movement was registered on the servo arm. Figure 35 shows the high-speed camera view.
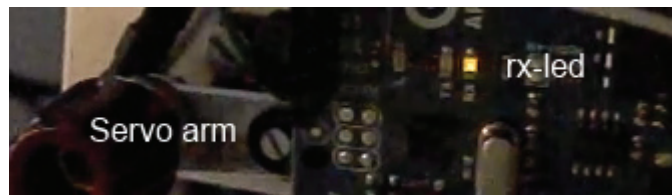
Figure 35: Image from high-speed camera with rx-led lit

From 50 samples, an average delay of 9.7 ms was found with delays ranging from 0.8 to 16.7 ms. This corresponds well with the theoretical delays of the PWM-control, and is something that has to be considered when discussing the results of the delay test. The Arduino operates at a clock speed of 16 MHz, and a quick test was conducted to measure the time it uses to generate output after receiving a serial command. The result can be seen in figure 36. From the figure, it can be seen that the Arduino only uses approx 50 μS, so in the context of the rest of the system, this delay is negligable.
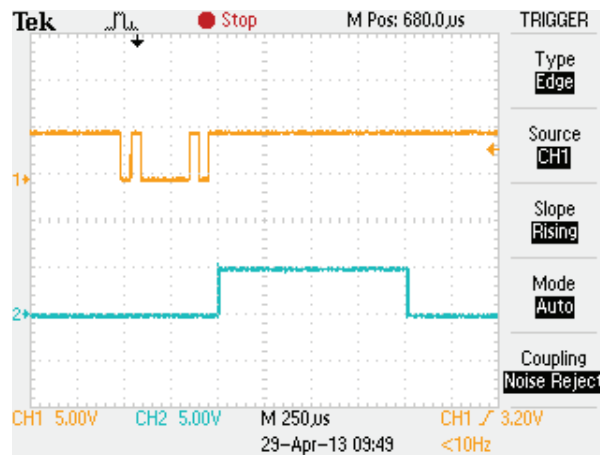
Figure 36: The delay in the Arduino between receiving a byte (top) and generating an output (bottom)

7.2   Delay Tests for ESWL Triggering System

17 samples were taken at St. Olavs Hospital. Screenshots from the oscilloscope were saved to a USB-stick and later analyzed. All the samples showed a delay of 32 ms. Figure 37 shows one of the screen shots. The top channel is the input from the trigger mechanism and the bottom channel shows the input from the microphone. The grid size is 10 ms.
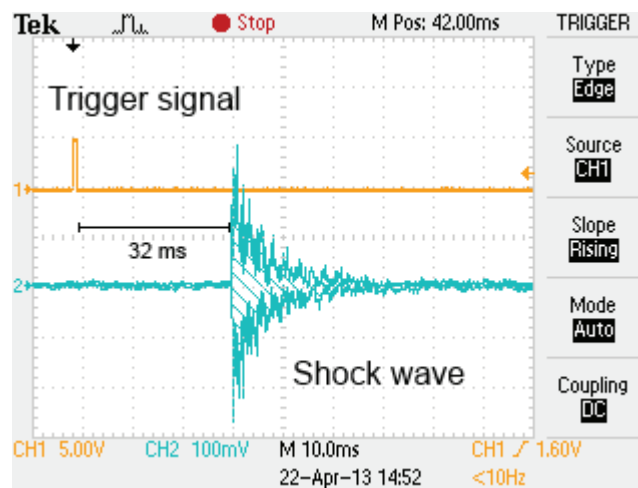
Figure 37: Oscilloscope screen-shot from the triggering delay test

Summary of the delay tests are shown in table 3. The lithotriptor manual stated a delay of 30-31 ms. The extra millisecond seen in the tests may have

51

come from the distance between the microphone and shock wave generator. However, compared to the delays of the imaging system, this is negligable.

Number of samples	17
Average delay	32 ms
Standard deviation	0 ms

Table 3: Results of the ESWL trigger delay test

7.2.1 Possible Sources of Error

A microphone and amplifier will introduce some errors in the measurement, as the amplifier may phase-shift the signal by a few degrees. The purpose of the test was to measure the time from triggering until a shock wave hitting the stone. The microphone was not placed inside the tank, as it was not water-proof, and hence the assumption was made that the difference in location would not cause a big difference in delay. The sound speed in water is approx 1500 $\frac{m}{s}$. This means that a displacement of, for instance, one meter would mean a delay difference of only 0.66 ms. Compared to the delay of the triggering, this is negligable.

7.3 Fragmentation Tests

After running the fragemntation tests the samples were numbered and packed for later analysis. At the university, each sample was dried in a coffee-filter and transferred to a small plastic container. The samples were later spread on a dark paper sheet and photographed.

7.3.1 Stationary- and Moving Stones

Figure 38 shows the fragmented stones. 5 stones were treated while stationary and 3 stones while moving. The aiming process was very difficult because if the small margins involved, especially for the moving stones. Combined with some time constraints when using the operating room, it lead to only running the movement tests on 3 stones. The differences between the moving and stationary stones are significant, which essentially means that more shockwaves hit the stationary stones.

53
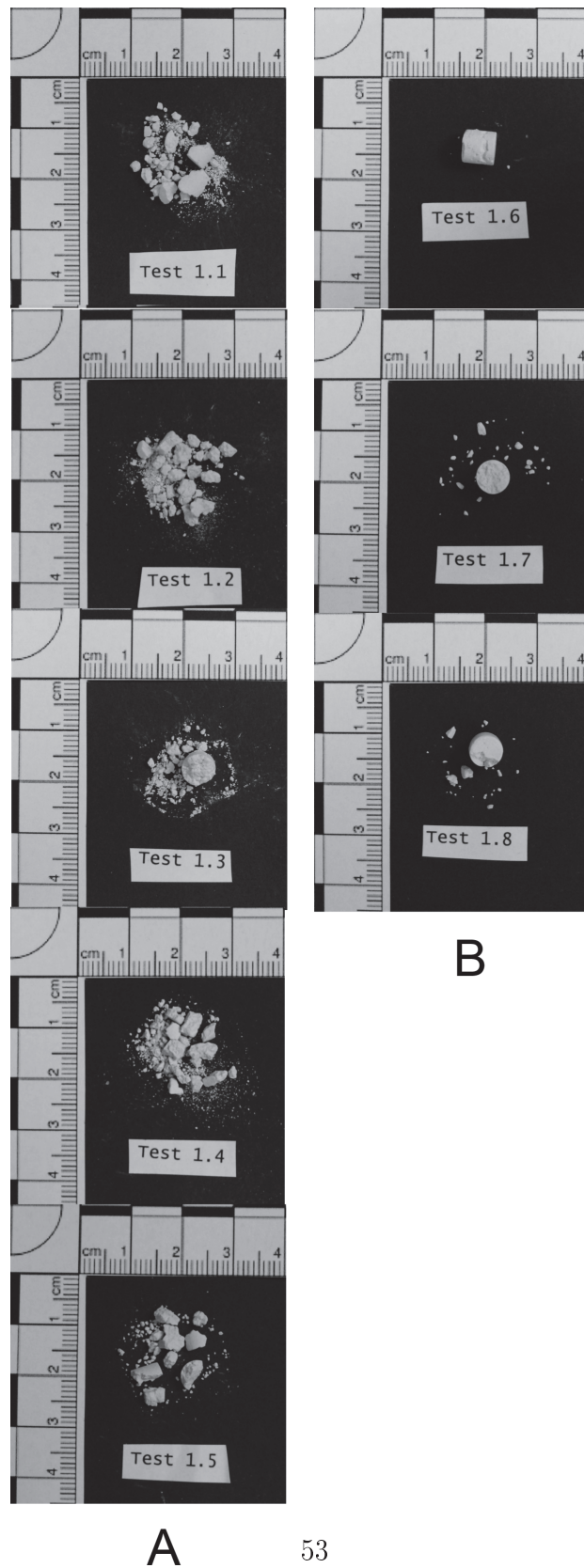
Figure 38: Column A: Stationary Stones Column B: Moving Stones

7.3.2   Real Stones vs. Model Stones

For the comparison test, a model stone was shaped to match the real stone
fragment obtained from St. Olavs Hospital. The stones, prior to fragmenta-
tion, can be seen in figure 39.

Figure 39: The real(left) and model(right) stone. The model stone was shaped
to look match the size of the real stone.

Figure 40 shows the same stones after receiving 600 shocks with energy setting
3.

Figure 40: Fragmented real(left) and model(right) stone

7.3.3   Possible Sources of Error

A big problem with these tests was the model stone positioning and movement
system. This system was based on the original system designed by Runnestø,
and improving this was not the aim of this thesis. A lot of time was spent on

getting the stone into the focal zone. The movement system also caused the moving stones paths to skew, making it difficult to make them pass through the focal zone. As a result of these inaccuracies in the simulator, a lot of time was spent using x-ray targeting to make small ajustments, and the x-ray system had to be reset several times because of a safety timer designed to protect the patient from excess x-ray exposure. These inaccuracies may have caused the moving stones to spend less than the theoretical 336 ms in the focal zone, and the stationary stones to not be completely in focus.

Air bubbles in the coupling gel between the water cushion and the flexible wall of the kidney tank may affect fragmenration, according to Jain et al.[8]. Some air bubbles were observed during the tests, and were hard to eliminate. However, the amount of air bubbles were roughly the same for all tests, so the impact should be somewhat equal.

8   Discussion

This section presents discussion around the functionality and delay of each of the system modules, and how they affect the full system.

The purpose of identifying the delays of the system modules, is to be able to design a predictor that can accurately overcome the delay. A predictor uses a model of the real system to predict future states and a-posteriori measurements to correct the model. Depending on the accuracy of the model and measurements, the length of the prediction horizon varies. If the delay is pre-calculated, as it is here, the predictor will use a fixed prediction length. This may cause problems if the real delay is not constant.

8.1   Imaging Module and Tracking Program

Using a framerate of 11 fps showed an average delay of 290 ms and the lowest standard deviation of the different framerates, but it still had a span from 177 ms up to 400 ms. However, 95 % of the samples were in the region 200 - 360 ms. If the prediction step is chosen to be in the middle of this 95 %-region, 280 ms, the actual delay will vary with ± 80 ms with 95 % confidence (based on the observed delay). If the stone spends 336 ms in the focal zone, as presented in section 6.3.1, and the predictor is able to estimate the center of the stones position, it will hit, even with the ± 80 ms jitter. From the center of the region, the stone will still be in sight for 168 ms, ($\frac{336}{2}$ms), which is more thant double the expected jitter in each direction. If this solution is to hold, it is assumed that the delay follows the same distribution as in the tests.

A comparison between the delays of the full imaging module + tracking system, and the delay of the tracking loop only, suggests that the biggest part of the delay come from the imaging module. The standard deviation of the tracking loop delay was also low, 5 ms for 11 fps, and this points to the imaging module for the high jitter as well.

It is difficult to identify what parts of the image module causes the delays and the jitter, as the system are run on two different computers, and the image transfer software, Ulterius, is not open source. During the testing, some dropped frames were experienced, which may be a result of the receiving PC not being able to process images fast enough. The delays experienced from the same tests in the authors previous thesis[40] were smaller. The tracking software were then run on a more powerful PC and this indicates that the delay is somewhat correlated with the performance of the PC hardware.

Based on the assuptions of stone movement above, the delay will not cause the system to fail, but real conditions may come with more constraints. The delay

of every module should ideally be as short and stable as possible. Because of the proprietary image tralsfer interface, it is difficult to make performance improvements here. Maybe another option should be considered, such as returning to the methohd used by Runnestø[36], a framegrabber. This solution is not as elegant as using a direct network transfer, but if the delay comes from the transfer and not the scanner itself, a framegrabber may be a better option.

It was identified in section 7.1.1 that the servo in the testing rig introduced a variable delay of 10 ms ± 10 ms because of its PWM control. This delay will not be experienced in a real treatment situation and the real jitter will therefore be less.

8.2   ESWL Trigger Module

The triggering modules designed and built, both functioned according to specifications. Because of the need to release individual shock waves with minimal delay, the dicision was made to use the ECG-trigger, because of the timing diagrams available in the documantation. Taking into account that this lithotriptor is not designed for releasing individual shock waves, the trigger module design was very successful and an integral part in completing the whole system.

The delay tests of the triggering module showed predictable delays, based on the available documentation. A delay of 30-31 ms was expected and the tests showed a constant delay of 32 ms. As mentioned in the test results, the extra millisecond in the delay may have been caused by the distance between the microphone and shock wave generator. Compared to the delays of the imaging module, this possible variation is very small. This part of the system is fairly simple, and because of the constant delay without jitter, this will not cause significant problems in predictor performance.

8.3   The Full System

When reviewing figure 16 in section 4.6 which summarizes the delays in the system, the observed delays can now be added.

The scanning and processing delay, image transfer delay and tracking algorithm delay were all tested in the image transfer delay tests. From the analysis in section 8.1 it was found that a delay of 280 ms ±80 ms delay was expected with a 95 % percent confidence. Subtracting the 10 ms average delay of the servo and the ±10 ms jitter, the result is 270 ms± 70 ms. Adding the delay of the triggering mechanism, the total delay is 302 ms ± 70 ms. Some delays

have not been measured, such as the time the PC uses from confirming the stone is in sight, until sending out the trigger signal, but this is assumed to be negligable because of the high processor speeds in a modern PC.

Runnestø used a predictor on tracking tests of pre recorded kidney movement [36]. He used two simple predictors, an extrapolated lowpass estimator, and a Kalman predictor, both based on a simple mivement model with a constant acceleration. He showed that the predictors had good performance on linear movements, but tended to overshoot when the stone turned. Since the predictors were based on a linear movement model, this is not unexpected. To improve the predictors, a more accurate model may be needed. This will be discussed in more detail in section 9.

As a result of the inaccuracies in the simulator tank making it hard to place the stone in the focal zone, and the fact that the ultrasound equipment available had a too shallow scan depth (9 cm), tests with the full system were not performed. The movement system for the model stones inside the tank, based on the original system by Runnestø, was very inaccurate as a result of the flexible rods required for the servo to move the stone. This made it close to impossible to make minor adjustments during x-ray to place the stone in focus. The decicion was therefore made that the movement system needs improvement, and better ultrasound equipment needs to be obtained before the complete system, with tracking enabled, can be tested.

8.4 Fragmentation of Stones

The fragmentaton tests consisted of two parts: Testing moving versus stationary stones, and model versus real stones. The purpose of the first set of tests was to show that fragmentation efficiency increased with an increasing number of hits on the stone. From the results in figure 38, a clear difference between the moving and stationary stones are seen. Some variations are present within each column, but this may have come from inaccurate aiming. The stones which have received all 600 shocks are heavily fragmented. Some of the samples still have fragments which are unpassable, however, compared to the column for the moving stones, the result is much better. Column B show stones almost in their original size, with some small fragments chipped off. The moving stones spent approx 2 x 336 ms in the focal zone, based on the movement pattern used, see section 6.3.1. This means that the stone is in focus only approx. 15% of the time. The movement may not be a realistic model of stone movement but it gives insight in how much movement affects fragmentation. This conforms with the results of previous research by Cleveland et al. [15]. In the context of the tracking system, these results suggests a big improvement in

fragmentation when using tracking, compared to no tracking, as the tracking system will enable more shots to hit the stone.

Conclusions about how many shocks are needed to break a real stone should not be drawn from this result. The model stone may be harder or more brittle than individual, real stones, and thus such a comparison is not correct. But is is assumed that real stones will exibit the same trends in diference in effectiveness of fragmentation when it comes to how many shots hit the stone.

The second part of the fragmentation tests were done to examine how a real stone is fragmented compared to a model stone when subjected to the same amount of shock waves. The test showed that the real kidney stone was fragmented into a mix of big and small pieces. The model stone in this test were not fragmented as much as the real one. A possible explanation is that the model stone was not targeted as good as the real one. When comparing the fragmentation of the real stone to the model stones fragmented in the first tests, results are similar. Because of very limite time available in the operating room when doing the last test, only one comparison test were done. However, the results support, combined with the literature, support that Ultracal-30 is suited for this kind of research and should be used in the test setup.

9   Further Work

One of the reasons for not being able to perform a full system test, was the lack of adequate ultrasound equipment. The scanner used in the delay tests had a too shallow and narrow scan depth (9 cm x 4 cm). It is neccesary to obtain a probe, or a whole system, with a wider and deeper scan. The kidney simulator tank measures 30 cm by 20 cm, and the probe should be able to scan 2/3 of the tank. If the system does not support the Ulterius interface for image transfer, a framegrabber can be used to transfer the images.

The delay and jitter of the imaging module were quite significant, compared to the rest of the system. Other ultrasound scanners and means of image transfer should be examined to see they show better real-time properties. One option is using a framegrabber, as done by Runnestø[36].

To enable the design of a customized predictor, knowledge about the movement patterns of kidney stones is needed. This task is well suited as a project for students of medicine. Videos should be recorded, more than the previous seven, and analyzed, to try to model the stones movement. It would also be interesting to find out if certain patient characteristics affect the movement, such as height, weight or age. A modified version of the tracking software could be used to track and log the stone movement in real time.

A task related to analyzing movement, is testing the performance of the tracking algorithm and usability of the program in real time, and this can be done in combination with the position logging. The system has previously only been testen on videos from real patients, so tests in real-time on real patients are needed. The target users of the system are medical personel, so the user-friendliness of the program should also be tested and ajustments made if aspects of the user interface need change.

Another task suited for students associated with the hospital is to gather statistics of ESWL treatment success, if this does not exist already. This data should include the success rate, as well as treatment details, stone and patient data. When the full system is ultimately tested on patients, data on the treatment success without the tracking system can be used for comparison.

From experiences during the fragmentation tests, it is clear that the kidney simulator tank and movement system need improvement to be able to conduct full system tests. Patients can easily be ajusted in all dimensions on the movable treatment table, but the simulator tank is supported by the therapy head, and therefore the stone must be moved inside the tank to place it in focus. Doing this by hand is a tedious process and involves a lot of x-ray exposure. This process should be remote controlled. A movement system that can be controlled in all dimensions is one option. The focusing process would

then be controlled from the computer with precise movements. If a 3D position regulator is implemented, positioning and complex movement patterns would be easy to perform. Another option is to fasten the tank to the arm which holds the treatment head. If the tank can be placed in a consistent position over the therapy head each time, the focal zone can be defined and marked inside the tank. With a sturdier movement system, which ensures that the stone follows the same path every time, only minor ajustments would be needed for each test. The drawback of this solution is that access to the lithotriptor is very limited as it is used for treatment every week. Regardless of which solution is chosen, it is clear that the simulator tank and movement system needs to be improved to enable full system tests.

The predictors used by Runnetsø showed decent performance, but also showed significant overshoots in the turning region of the stone. Other, more advanced and customized predictors should be developed and tested to see if better performance may be achievable. Using prediction to aid real time tracking of moving objects inside the body, where the movement is respiration induced, has been researched by others. Sharp et al.[20] presents results from tracking tumors for real time-guided radiotherapy. As in the system presented here, delays because of limited framerates, computation and communication exist, and makes the dose delivery potentially inaccurate. They present results from using several predictors, linear, Kalman and Artificial Neural Networks. The predictors parameters, such as the matrices A, B, Q and R for a Kalman filter are found during a training phase using optimization on training data for each patient. This makes the predictors customized for each different breathing pattern and movement excursion. Their results suggest that predictors will have better performance than no prediction in most cases, especially when the delay is long (1 second) or the framerate is low (3 Hz). A similar approach is shown by Jung et al.[10] where the system is modeled using a the "Local Circular Motion"-model, and an extended Kalman filter is used for prediction. This is an advanced version of a Kalman filter for nonlinear systems. The results show that this filter is able to predict respiratory motion. It is desirable to find out if these prediction methods ans models can be transferred for use in modeling and prediction of kidney stone movement.

An important step in making the system usable on real patients is synchronizing the focal point between the lithotriptor and ultraosound equipment. Ultrasound guidance is an option on the Dornier Compact Delta, but this equipment was not available at St. Olavs Hospital. The optional ultrasound equipment are mounted on an isocentric arm next to the treatment head, which means that it can only move aimed around a single point, the focal point. The point is then visible on the ultrasound screen. Obtaining this equipment is

the easiest way of synchronizing the focal point. Another approach is fitting an ultrasound probe with markers visible to a stereoscopic camera which can track its position and heading. The focal point may then be programmed as part of the model relative to the lithotriptor. This method is used on the Sonolith i-Move, which is a modern lithotriptor system[43]. Here, the stone is found using a free ultrasound probe with markers. Since the probe is tracked in 3D, the system knows the coordinates of the stone once it is found by an operator, and the patient table is ajusted automatically to place the stone in focus. This system is more adcanved and versatile, but it involves alot more equipment and software than the simple isocentric arm mount.

The full system with tracking has not yet been tested, so this is an obvious point on the further work agenda. As mentioned above, some parts of the system should be improved to make tests easier and more accurate such as the simulator tank and ultrasound equipment. If the tests are performed on the simulator tank, ultrasound focal point integration may not be needed as the stone can be placed in the focal point using x-ray and the focal point defined in ultrasound based on the stones position. This solution requires a stable simulator tank and probe. For tests on real patients, integration is needed as the stone is not stationary.

9.1 Further Work Summary

The propositions for further work are summarized in the following bulletpoints:

- Obtain ultrasound equipment with sufficient scan depth and width

- Examine the delays of other ultrasound scanners and means of image transfer

- Investigate kidney stone movements in real patients in a treatment setting using ultrasound imaging

- Test tracking system performance on real patients (independent of ESWL treatment)

- Gather statistics on treatment success for patients treated with ESWL at St. Olavs Hospital

- Improve movement and positioning system for the phantom stones and mount stability for the simulator tank

- Based on the movement patterns and delays, design a customized predictor to overcome the delay

- Find a way to synchronize the focal point between the lithotriptor and the ultrasound imaging system

- Test the full system using the kidney simulator tank

- Test the full system on real patients

10   Conclusion

The work presented in this thesis is a continuation of work presented in two previous master theses and two project theses.

A literary study was first carried out, to survey research covering parameters affecting ESWL treatment results. The processes involved in fragmentation can be summarized to two main processes, stress waves and cavitation. Many parameters affect fragmentation, but the most important one, in the context of this thesis, is stone movement. It is estimated that more than 50% of shock waves miss the stone during normal treatment. Shock waves missing the stone, cause damage to surrounding tissue, and prolongs treatment time, as more shock waves are required ot fragment the stone.

A tracking program was developed as part of previous work. To test this system, a complete test setup is needed. The test setup presented in this thesis is a combination of previously created modules (tracking program, kidney simulator tank) and modules developed here to complete the setup (ESWL-control unit, model stones). The kidney simulator tank was also augmented with two flexible walls. All the modules were tested to verify their usability and compatibility. Both the new kidney simulator tank and the ESWL triggering mechanism were verified to work at St. Olavs Hospital. Since the system will need prediction to be able to target the stone, the delay of each part of the chain were analyzed.

The imaging module showed the biggest delay, combined with a high standard deviation. From the samples taken, it was calculated that the imaging module and tracking systems worst case delay was 270 ms $\pm$ 70 ms. The delay of the triggering system was found to be approx. 32 ms, as expected from the manual. This add up to a total system delay of 302 ms$\pm$ 70 ms with 95 % confidence based on the samples.

As presented in the discussion, the jitter would not make shock waves miss the stone when following the assumed movement pattern. However, this may not hold for moving stones in real patients.

The purpose of the fragmentation tests was to show the difference in efficiency when treating stationary stones compared to moving ones. 5 stationary stones and 3 moving stones were subjected to the same amount of shock waves of the same intensity. The moving stones showed much less fragmentation, the stones were almost of their original size with only a few small pieces chipped off. The stationary stones were fragmented into pieces of varying size, some as small as grains of sand, and others too large to pass naturally. Since the stones cannot be directly compared to real stones, the point is not to determine how many shocks are needed to treat the stones. The results strongly suggest that

stones receiving more shocks, i. e. the stationary stones, are more fragmented. Therefore, a tracking system enabling every shot to hit, should achieve a more effective fragmentation than normal treatment.

During testing, some problems of aiming with the kidney simulator tank were identified. Combined with the fact that available ultrasound equipment were inadequate(too shallow scan depth), the decision was made that the full system, with tracking, was not ready to be tested until some of the modules have been improved and better ultrasound equipment has been obtained.

References

[1] Avantgarde urology: Kidney stones http://www.avantgardeurology.com/c-k-kidney-stones-en.html.

[2] *Dornier MedTech Dornier Compact Delta Operating Manual Revision: K Number: K1025516.*

[3] *Dornier MedTech Service Manual Control Unit.*

[4] *Dornier MedTech Service Manual Shock Wave Circuit.*

[5] Haim Matzkin Alexander Greenstein. Does the rate of extracorporeal shock wave delivery affect stone fragmentation? *Adult Urology*, 54:430–432, 1999.

[6] Lawrence A. Crum Mary Dyson Andrew J. Coleman, John E. Saunders. Accoustic cavitation generated by an extracorporeal shockwave lithotripter. *Ultrasound in Medicine and Biology*, 13:69–76, 1987.

[7] Gopal Badlani Louis Kavoussi Arthur D. Smith, Glenn Preminger. *Smith's Textbook of Endourology*. Wiley-Blackwell, 2012.

[8] Tariq K. Shah Arun Jain. Effect of air bubbles in the coupling medium on efficacy of extracorporeal shock wave lithotripsy. *European Urology*, 51:1680–1687, 2007.

[9] Christian Bach, Theocharis Karaolides, and Noor Buchholz. Extracorporeal shockwave lithotripsy: What is new? *Arab Journal of Urology*, 10:289–295, 2012.

[10] Sun-Mog Hong Bo-Hwang Jung, Byoung-Hee Kim. Respiratory motion prediction with extended kalman filters based on local circular motion model. *International Journal of Bio-Science and Bio-Technology*, 5:51–58, 2013.

[11] E. Shmiedt CH. Chaussy, Walter Brendel. Extracorporeally induced destruction of kidney stones by shock waves. *The Lancet*, December 13:1265–1268, 1980.

[12] C. C. Chang, S. M. Liang, Y. R. PU, C. H. Chen, I. Manousakas, T. S. Chen, C. L. Kuo, F. M. Yu, and Z. F. Chu. In vitro study of ultrasound based real-time tracking of renal stones for shock wave lithotripsy: Part 1. *The Journal of Urology*, 166:28–32, 2001.

[13] C. C. Chang, S. M. Liang, Y. R. PU, C. H. Chen, I. Manousakas, T. S. Chen, C. L. Kuo, F. M. Yu, and Z. F. Chu. In vitro study of ultrasound based real-time tracking of renal stones for shock wave lithotripsy: Part ii-a simulated animal experiment. *The Journal of Urology*, 167:2594–2597, 2002.

[14] Bernd Forsmann Christian Bohris Andreas Lutz Martine Tailly-Cusse Thomas Tailly Christian Chaussy, Geert Tailly. Extracorporeal shock wave lithotripsy in a nutshell.

[15] Robin O. Cleveland, Ronald Anglade, and Richard K Babayan. Effect of stone motion on in vitro comminution efficiency of storz modulith slx. *Journal of Endourology*, 18:629–633, 2004.

[16] S. S. Dhara D. J. Cantry. High frequency jet ventilation through a supra-glottic airway device: a case series of patients undergoing extra-corporeal shock wave lithotripsy. *Journal of the Association of Anaesthetists of Great Britain and Ireland*, 64:1295–1298, 2009.

[17] Wolfgang Eisenmenger. The mechanisms of stone fragmentation in eswl. *Ultrasound in Medicine and Biology*, 27:683–693, 2001.

[18] Murad Basar Devrim Tuglu Cagatay Mert Halil Basar Erdal Yilmaz, Ertan Batislam. Optimal frequency in extracorporeal shock wave lithotripsy: Prospective randomized study. *Adult Urology*, 66:1160–1164, 2005.

[19] Julia Carrasco-Valiente Fernando Anaya-Henares Jose Luis Carazo-Carazo Jose Alvarez-Kindelán Juan Carlos Regueiro-López Maria Jose Requena-Tapia Francisco Jose Anglada-Curado, Pablo Campos-Hernández. Extracorporeal shock wave lithotripsy for distal ureteral calculi: Improved efficacy using low frequency. *International Journal of Urology*, 2012.

[20] Shinichi Shimizu Hiroki Shrato Gregory C Sharp, Steve B Jiang. Prediction of respiratory tumor motion for real-time image-guided radiotherapy. *Physics in Medicine and Biology*, 49:425–440, 2004.

[21] Phillip Eisenberg http://web.mit.edu/hml/ncfmf/16CAV.pdf. Cavitation.

[22] Chien-Chen Chang Shen-Min Liang Ioannis Manousakas, Yong-Ren Pu. Ultrasound image analysis for renal stone tracking during extracorporeal shock wave lithotripsy. *Proceedings of the 28th IEEE EMBS Annual International Conference*, pages 2746–2750, 2006.

[23] Robin O. Cleveland Javies Van Cauwelaert Michael R. Bailey-David A. Lifshitz-Andrew P. Evan James A. McAteer, James C. Williams Jr. Ultracal-30 gypsum artificial stones for research on the mechanisms of stone breakage in shock wave lithotripsy. *Urological Research*, 33:429–434, 2005.

[24] Noel Sankey Paramjit S. Chanhoke Job Chacko, Michael Moore. Does a slower traeatment rate impact the efficacy of extracorporeal shock wave lithotripsy for solitary kidney or ureteral stones? *The Journal of Urology*, 175:1370–1374, 2006.

[25] Melanie Harju University of Toronto Lithotripsy Associates R. John D'a Honey Kenneth T. Pace, Daniela Giculete. Shock wave lithotripsy at 60 or 120 shocks per minute: A randomized, double-blind trial. *The Journal of Urology*, 174:595–599, 2005.

[26] Brian R. Matlaga Michelle Jo Semins, Bruce J. Trock. The effect of shock wave rate on the outcome of shock wave lithotripsy: A meta-analysis. *The Journal of Urology*, 179:194–197, 2008.

[27] Bradford Sturtevant Murtuza Lokhandwalla. Fracture mechanics model of stone communition in eswl and implications for tissue damage. *Physics in Medicine and Biology*, 45:1923–1940, 2000.

[28] T. G. Hertz A. Holm E. Lindstedt H. W. Persson-C. H. Hertz N.-G. Holmer, L.-O Almquist. On the mechanism of kidney stone disintegration by accoustic shock waves. *Ultrasound in Medicine and Biology*, 17:479–489, 1991.

[29] P. Zhong N. Smith. Stone communition correlates with the average peak pressure incident on a stone during shock wave lithotripsy. *Journal of Biomechanics*, 45:2520–2525, 2012.

[30] Brian MacConaghy Michael R. Bailey Oleg A. Sapozhnikov, Adam D. Maxwell. A mechanistic analysis of stone fracture in lithotripsy. *Journal Acoustic Society of America*, 121:1190–2002, 2007.

[31] Michael R. Bailey James C. WIlliams Jr James A. McAteer-Robin O. Cleveland-Lawrence A. Crum Oleg A. Sapozhnikov, Vera A. Khlokhlova.

Effect of overpressure and pulse repetition frequency on cavitation in shock wave lithotripsy. *Journal Acoustic Society of America*, 112:1183–1195, 2002.

[32] M. Orkisz, M. Bourlion, G. Gimenez, and T. A. Flam. Real-time target tracking applied to improve fragmentation of renal stones in extra corporeal lithotripsy. *Machine Visioned and Applications*, 11:138–144, 1999.

[33] Maciej Orkisz, Teymour Farchtchian, Djillali Saighi, Maurice Bourlion, Nicolas Thiounn, Gerard Gimenez, Bernard Debre, and Thierry A. Flam. Image based renal stone tracking to improve efficiancy in extracorporeal lithotripsy. *The Journal of Urology*, 160:1237–1240, 1998.

[34] Jens J. Rassweiler, Thomas Knoll, Kai-Uwe Köhrmann, James A. McAteer, James E. Lingemann, Robin O. Cleveland, Michael R. Bailey, and Christian Chaussy. Shock wave technology and application: An update. *European Urology*, 59:784–796, 2011.

[35] Jostein Låg Runnestø. Ultralydfantom for knusing av nyrestein, project thesis. NTNU, Institutt for Teknisk Kybernetikk, 2010.

[36] Jostein Låg Runnestø. Sanntidssporing av nyrestein. Master's thesis, NTNU, Institutt for Teknisk Kybernetikk, 2011.

[37] James E. Lingeman Andrew P. Evan Bret A. Connors Naomi S. Fineberg James C. Williams Jr James A. McAteer Ryan F. Paterson, David A. Lifshitz. Stone fragmentation during shock wave lithotripsy is improved by slowing the shock rate: Studies with a new animal model. *The Journal of Urology*, 168:2211–2215, 2002.

[38] 2013. Web. 12 Feb. 2013. http://www.britannica.com/EBchecked/topic/541339/shockwave "shock wave." Encyclopædia Britannica. Encyclopædia Britannica Online Academic Edition. Encyclopædia Britannica Inc.

[39] Glenn M. Preminger Pei Zhong Songlin Zhu, Franklin H. Cocks. The role of stress waves and cavitation in stone comminution in shoch wave lithotripsy. *Ultrasound in Medicine and Biology*, 28:661–671, 2002.

[40] Johan Markus Steinholt. Guiding equipment used for fragmentation of kidney stones, integration of ultrasound imaging equipment and control unit.

[41] Palaniappan Sundaram and Yeh Hong Tan. Minimally invasive surgical and medical management of urinary calculi. *Proceedings og Singapore Healthcare*, 2:120–124, 2012.

[42] Martha K. Terris. Pyelolithotomy treatment & management, http://emedicine.medscape.com/article/448503-treatment.

[43] EDAP TMS. Sonolith i-move brochure http://www.edap-tms.com/uploads/pdf/sonoliht-i-move-v2-2011.pdf.

[44] Jens Kristian Tøraasen. Sanntids følging av nyrestein i ultralydavbildning. Master's thesis, NTNU, Institutt for Teknisk Kybernetikk, 2010.

[45] Kjell Tveter and Rolf Wahlqvist. nyrestein (store medisinske leksikon). i store norske leksikon.

[46] C. Tang S. Zhao Y. Wang F. Rong D. Dai M. Guan A. Qi W. Eisenmenger, X. X. Du. The first clinical results of "wide-focus and low-pressure" eswl. *Ultrasound in Medicine and Biology*, 28:769–774, 2002.

[47] Hans-Petter Dreyer Eike Matura Walter Folberth Hans-Georg Priesmeyer Jürgen Seifert Wolfgang Sass, Martin Braünlich. The mechanisms of stone disintegration by shock waves. *Ultrasound in Medicine and Biology*, 17:239–243, 1991.

[48] Glenn M. Preminger Pei Zhong Yufeng Zhou, Franklin H. Cocks. The effect of treatment strategy on stone communition efficiency in shock wave lithotripsy. *The Journal of Urology*, 172:349–354, 2004.

[49] Pei Zhong Yunbo Liu. Begostone - a new stone phantom for shock wave lithotripsy research. *Accoustical Society of America*, 112:1265–1268, 2002.

Appendix

Appendix A: CD Contents

- Refrence papers

- PDF-version of this thesis

- Arduino IDE and Compiler

- Arduino source code

Appendix B: Arduino Source Code

Arduino version: 1.0.3

ESWL-control

```
1  /* This program sends out the ESWL trigger signal
2  when receiving the char 'A' through serial
3  */
4
5  //Output PIN for the ECG-signal
6  int outPin = 12;
7  byte receivedData;
8
9  void setup() {
10     pinMode(outPin, OUTPUT);
11     //Initiate serial
12     Serial.begin(19200);
13  }
14  void loop() {
15     if(Serial.available()>0){
16         receivedData = Serial.read();
17         //Sends trigger signal if the char 'A' is received
18         if(receivedData == 'A'){
19             //Create the 1ms 5V pulse
20             digitalWrite(outPin, HIGH);
21             delayMicroseconds(1000);
22             digitalWrite(outPin, LOW);
23         }
24     }
25  }
```

Simulator Movement Control

```
1  /* This program is controlled via Serial.
2  Each command is a single character.
3  Commands:
4  'c': Set servo to start pos
5  'r': Start movement
6  's': Stop movement and return servo to start pos
7  */
8
9  #include <Servo.h>
10 #include <MsTimer2.h>
11
12 Servo servo1;
13 int state = (int)'c';
14 int easing_value = 125;
15 int last_pos = 0;
16 boolean easing_init = false;
17 const int resp_per_minute = 14;
18 const int tableEntries = 252;
19 const int timerInMillies = (int)((60000/resp_per_minute)/
     tableEntries);
20 const int sinusLookupTable[] = {EXCLUDED HERE FOR VISUAL
     PURPOSES, SEE CODE ON CD}
21 int currentIndex = 0;
22
23 void setup() {
24     servo1.attach(9, 900, 2100);
25     Serial.begin(19200);
26     setupTimer2();
27 }
28
29 void setupTimer2() {
30     MsTimer2::set(timerInMillies, move);
31     MsTimer2::start();
32 }
33
34 void move() {
35     if(Serial.available()>0){
36         state = Serial.read();
37     }
38
39     switch(state){
40         //Move servo to start pos
41         case (int)'c':
42         servo1.write(125);
43         break;
44
45         //Start movement
```

```
46          case (int)'r':
47              if(currentIndex == tableEntries) {
48              currentIndex = 0;
49              }
50              servo1.write(sinusLookupTable[currentIndex]);
51              currentIndex++;
52              break;
53
54              //Stop movement and return servo to start pos
55          case (int)'s':
56              if(currentIndex == tableEntries) {
57                  currentIndex = 0;
58              }
59              if(sinusLookupTable[currentIndex] == 125) {
60              state = (int)'c';
61              }
62              servo1.write(sinusLookupTable[currentIndex]);
63              currentIndex++;
64              break;
65      }
66 }
67
68 void loop(){;}
```